Journal of Artificial Intelligence Research 72 (2021) 759-818 Submitted 03/2021; published 11/2021

Multi-Label Classification Neural Networks with Hard Logical Constraints

Eleonora Giunchiglia ELEONORA.GIUNCHIGLIA@CS.OX.AC.UK
Department of Computer Science,
University of Oxford, UK

Thomas Lukasiewicz THOMAS.LUKASIEWICZ@CS.OX.AC.UK
Department of Computer Science,
University of Oxford, UK

Abstract

Multi-label classification (MC) is a standard machine learning problem in which a data point can be associated with a set of classes. A more challenging scenario is given by hierarchical multi-label classification (HMC) problems, in which every prediction must satisfy a given set of hard constraints expressing subclass relationships between classes. In this article, we propose C-HMCNN(h), a novel approach for solving HMC problems, which, given a network h for the underlying MC problem, exploits the hierarchy information in order to produce predictions coherent with the constraints and to improve performance. Furthermore, we extend the logic used to express HMC constraints in order to be able to specify more complex relations among the classes and propose a new model CCN(h), which extends C-HMCNN(h) and is again able to satisfy and exploit the constraints to improve performance. We conduct an extensive experimental analysis showing the superior performance of both C-HMCNN(h) and CCN(h) when compared to state-of-the-art models in both the HMC and the general MC setting with hard logical constraints.

1. Introduction

Multi-label classification (MC) is a standard machine learning problem in which a data point can be associated with a set of classes. A more challenging scenario is given by hierarchical multi-label classification (HMC) problems, in which every prediction must satisfy a given set of hard hierarchy constraints of the form

$$A_1 \to A, \tag{1}$$

expressing that A_1 is a subclass of A, that is, that if a data point is associated with the class A_1, then it is also associated with the class A. HMC problems naturally arise in many domains, such as image classification (Deng et al., 2009; Dimitrovski et al., 2008, 2012), text categorization (Klimt & Yang, 2004; Lewis et al., 2004; Rousu et al., 2006), and functional genomics (Barutcuoglu et al., 2006; Clare, 2003; Vens et al., 2008). They are very challenging for two main reasons: (i) they are normally characterized by a great class imbalance, because the number of data points per class is usually much smaller at deeper levels of the hierarchy, and (ii) the predictions must be coherent with (i.e., satisfy) the hierarchy constraints. Consider, for example, the task proposed by Dimitrovski et al. (2008), where a radiological image has to be annotated with an IRMA code specifying, among others, the biological system examined. In this setting, we expect to have many more *abdomen* images than *stomach* images, making the class *stomach* harder to predict. Furthermore, the prediction {*stomach*} alone should not be possible given the constraint

$$\textit{stomach} \rightarrow \textit{gastrointestinalSystem}, \tag{2}$$

stating that the stomach is part of the gastrointestinal system, that is, that whenever *stomach* is predicted, also *gastrointestinalSystem* should be. Many models have been specifically developed for HMC problems, and we can distinguish those that directly output predictions that are coherent with the hierarchy constraints (see, e.g., Bi & Kwok, 2011; Masera & Blanzieri, 2018) from those that allow incoherent predictions and, at inference time, require an additional post-processing step to ensure their satisfaction (see, e.g., Cerri et al., 2014; Obozinski et al., 2008; Valentini, 2011). Most of the state-of-the-art HMC models based on neural networks belong to the second category (see, e.g., Cerri et al., 2014, 2016; Wehrmann et al., 2018), and different post-processing techniques can be applied in order to guarantee the coherency of their outputs with the constraints (see, e.g., Obozinski et al., 2008).

In this article, we first focus on HMC problems, and we propose a novel approach for solving them, called *coherent hierarchical multi-label classification neural network* (C-HMCNN(h)), which, given a network h for the underlying MC problem, exploits the hierarchy information to produce predictions coherent with the hierarchy constraints and improve performance. C-HMCNN(h) is based on two basic elements:

1. a constraint layer built on top of h, which extends to the upper classes the predictions made by h on the lower classes in the hierarchy, in order to ensure that the final outputs are coherent by construction with the hierarchy constraints, and

2. a loss function teaching C-HMCNN(h) when to exploit the hierarchy constraints, that is, when the prediction on the lower classes in the hierarchy can be exploited to make predictions also for the upper ones.

C-HMCNN(h) significantly differs from previous approaches for HMC problems based on neural networks. Indeed, the constraint layer is not a simple post-processing meant to guarantee the satisfaction of the hierarchy constraints, decoupled from the rest of the system. In C-HMCNN(h), the constraint layer and the underlying neural network h are tightly integrated, and it does not make sense to modify the constraint layer without modifying the way in which h is trained.

Secondly, we extend the language used to express the hierarchy constraints (1) to allow for the specification of more complex logical relations among classes. Indeed, the language for expressing hierarchy constraints is very limited, and it is not expressive enough to model, for example, the fact that if a medical image contains the abdomen but neither the middle nor the upper abdomen, then it contains the lower abdomen. Thus, borrowing concepts from the area of logic programming, we consider general constraints expressed as normal rules (Lloyd, 1987), that is, expressions of the form:

$$A_1, \ldots, A_k, \neg A_{k+1}, \ldots, \neg A_n \rightarrow A, \qquad (0 \leq k \leq n), \tag{3}$$

which imposes that whenever the classes $A_1, \dots, A_k$ are predicted, while $A_{k+1}, \dots, A_n$ are not, then also the class A should be predicted. Such constraints generalize hierarchy constraints (corresponding to the case $n = k = 1$) and naturally arise in many application domains like healthcare. With such an extension, we can now write:

$$abdomen, \neg middleAbdomen, \neg upperAbdomen \to lowerAbdomen,$$

capturing the above informally stated constraint. We call MC problems with a set of constraints in such an extended syntax *logically constrained multi-label classification* (LCMC) problems. By restricting to constraints with stratified negation (Apt et al., 1988), given a set $\mathcal{H}$ of initial predictions made by an underlying model h, we show how at inference time it is possible to compute in linear time in the number of constraints the unique minimal set of classes $\mathcal{M}$ that

1. extends $\mathcal{H}$, that is, such that $\mathcal{H} \subseteq \mathcal{M}$, and
2. is coherent with (satisfies) the constraints, that is, such that, given (3), $A \in \mathcal{M}$ whenever $\{A_1, \dots, A_k\} \subseteq \mathcal{M}$ and $\{A_{k+1}, \dots, A_n\} \cap \mathcal{M} = \emptyset$.

Indeed, for a non-stratified set of constraints expressed as normal rules, there can be no or more than one minimal set of classes having the above two properties, and determining the non-existence or computing one of them can take exponential time. We thus propose a novel model called *coherent-by-construction network* CCN(h), which is the first model able to deal with MC problems with such expressive constraints on the classes. CCN(h) has the same two basic ingredients of C-HMCNN(h):

1. a constraint layer built on top of h, which extends the predictions made by h in order to ensure that the predictions are coherent by construction with the constraints, and
2. a loss function, teaching CCN(h) when to exploit the constraints, that is, in the presence of (9), when to exploit the prediction on $\{A_1, \dots, A_n\}$ to make predictions on A.

In CCN(h), like in C-HMCNN(h), the constraint layer and h are tightly integrated, and the result is a system that significantly differs from what we consider the standard approach to LCMC problems, consisting in applying the constraint layer as a simple post-processor to a state-of-the-art MC system.

From a higher perspective, the core idea behind our approach is (i) to build models based on neural networks in order to leverage their learning abilities, (ii) to incorporate the constraints in the models themselves in order to guarantee their coherency with the constraints by construction, and (iii) to exploit the background knowledge expressed by the constraints by suitably modifying the loss function in order to improve performance. As such, our approach represents a valid alternative to the currently deployed techniques for certifying that a neural network model behaves correctly with respect to a given set of requirements expressed as normal rules. Such certification process – see the survey by Huang et al. (2020) – is mandatory especially in safety-critical applications, and is currently based on (i) verification techniques (see, e.g., Pulina & Tacchella, 2010; Lomuscio & Maganti, 2017), which suffer from a scalability problem, or (ii) testing techniques (see, e.g., Pei et al., 2019; Ma et al., 2018), which cannot give any guarantee that the model does always satisfy the constraints. Our approach, on the contrary, presents neither of the above limitations.

The main contributions of this article can thus be briefly summarized as follows:

- We propose a novel model for HMC problems, denoted C-HMCNN(h), and a novel model for LCMC problems, denoted CCN(h), which we prove to be an extension of C-HMCNN(h).
- We prove that CCN(h)'s predictions are guaranteed to be coherent with the constraints expressed as normal rules, and hence that C-HMCNN(h)'s predictions are guaranteed to be coherent with the hierarchy constraints.
- We show that CCN(h) (and hence C-HMCNN(h)) can be implemented on GPUs using standard libraries.
- We perform an extensive experimental analysis on 38 real-world datasets, showing that CCN(h) outperforms the current state-of-the-art models on both HMC and LCMC problems.

This article is a substantial extension of the work by Giunchiglia and Lukasiewicz (2020), which deals only with hierarchy constraints and presents C-HMCNN(h).

The rest of this article is organized as follows. In Section 2, we first focus on HMC problems, and we propose our model C-HMCNN(h). In Section 3, we consider more expressive constraints and present our model CCN(h), which extends C-HMCNN(h) to handle LCMC problems. The implementation of both C-HMCNN(h) and CCN(h) on GPUs is presented in Section 4. The experimental analysis, demonstrating the superiority of our approach, is reported in Section 5. We end the article with the relevant related work in Section 6 and the conclusion in Section 7.

2. Hierarchical Multi-Label Classification

In this section, we first introduce some basic definitions in hierarchical multi-label classification (HMC). We then describe the main intuitions underlying our model C-HMCNN(h) to solve HMC problems along a simple HMC problem with just two classes, and we finally present our general approach to solve HMC problems.

2.1 Preliminaries

A *multi-label classification* (*MC*) problem $\mathcal{P}$ is a pair $(\mathcal{A}, \mathcal{X})$ where $\mathcal{A}$ is a finite set of *classes* (also called *class labels* or simply *labels*), denoted by $A, A_1, A_2, \ldots$, and $\mathcal{X}$ is a finite set of pairs (x, y) where $x \in \mathbb{R}^D (D \geq 1)$ is a *data point*, and $y \subseteq \mathcal{A}$ is the *ground truth* of x, that is, the set of classes associated with x. A *model* m for $\mathcal{P}$ is a function $m(\,\cdot\,,\,\cdot\,)$ mapping every class A and every data point $x \in \mathbb{R}^D$ to $[0, 1]$. For every class A, the function $m_A \colon \mathbb{R}^D \to [0, 1]$ is defined by $x \mapsto m(A, x)$, for every data point $x \in \mathbb{R}^D$. A data point $x \in \mathbb{R}^D$ is *predicted* by m to belong to class A whenever $m_A(x)$ is greater than a user-defined *threshold* $\theta \in [0, 1]$.

A *hierarchical multi-label classification* (*HMC*) problem $(\mathcal{P}, \Pi)$ consists of an MC problem $\mathcal{P}$ and a finite set Π of *(hierarchy) constraints* of the form

$$A_1 \to A, \tag{4}$$

where A_1 and A are classes, such that the graph associated to Π with an edge from A_1 to A for each such constraint in Π is acyclic. Informally, given an HMC problem $(\mathcal{P}, \Pi)$, a model m for $(\mathcal{P}, \Pi)$ has to be coherent with the hierarchy constraints Π in $\mathcal{P}$, that is, m has to predict A whenever it predicts A_1, for each constraint (4) in Π. This is formally defined as follows.

Definition 2.1. Let $(\mathcal{P}, \Pi)$ be an HMC problem. Let m be a model for $\mathcal{P}$. If for a data point and for a constraint $A_1 \to A$ in Π, m predicts A_1 but not A, then m commits a *logical violation*. If m commits no logical violations, then m is *coherent with respect to* Π.

Given the above, whenever a model m is not guaranteed to satisfy a constraint (4), m is extended with a post-processing step to enforce $m_A(x) > \theta$ whenever $m_{A_1}(x) > \theta$ (Cerri et al., 2014; Obozinski et al., 2008; Valentini, 2011). However, it is often common practice to require the stronger condition $m_{A_1}(x) \leq m_A(x)$, and the falsification of this condition is referred to as hierarchy violation (Vens et al., 2008; Wehrmann et al., 2018).

Definition 2.2. Let $(\mathcal{P}, \Pi)$ be an HMC problem. Let m be a model for $\mathcal{P}$. If for a data point x and a constraint $A_1 \to A$ in Π, $m_{A_1}(x) > m_A(x)$, then m commits a *hierarchy violation*.

If a model commits no hierarchy violations, then it also commits no logical violations (and so is coherent relative to the constraints), while the converse does not necessarily hold.

For ease of presentation, we often omit the dependency from data points, and simply write, for example, m_A instead of $m_A(x)$.

2.2 Basic Case

Our goal is to leverage standard neural network approaches for MC problems and then exploit the hierarchy constraints in order to produce coherent predictions and improve performance. Given our goal, we first present two basic approaches, exemplifying their respective strengths and weaknesses. These are useful to then introduce our solution, which is shown to present their advantages without exhibiting their weaknesses. In this section, we assume to have just two classes A_1, A and the constraint (4).

In the first approach, we treat the problem as a standard multi-label classification problem and simply set up a neural network f with one output per class to be learned: to ensure that no hierarchy violation happens, we need an additional post-processing step. In this simple case, the post-processing could set the output for A_1 to be $\min(f_{A_1}, f_A)$ or the output for A to be $\max(f_A, f_{A_1})$. In this way, all predictions are always coherent with the hierarchy constraint. A second approach is to build a network g with two outputs, one for A_1 and one for $A \setminus A_1$. To meaningfully ensure that no hierarchy violation happens, we need an additional post-processing step in which each prediction for the class A is given by $\max(g_{A \setminus A_1}, g_{A_1})$. Considering the two above approaches, depending on the specific distribution of the data points, one solution may be significantly better than the other, and a priori we may not know which one it is.

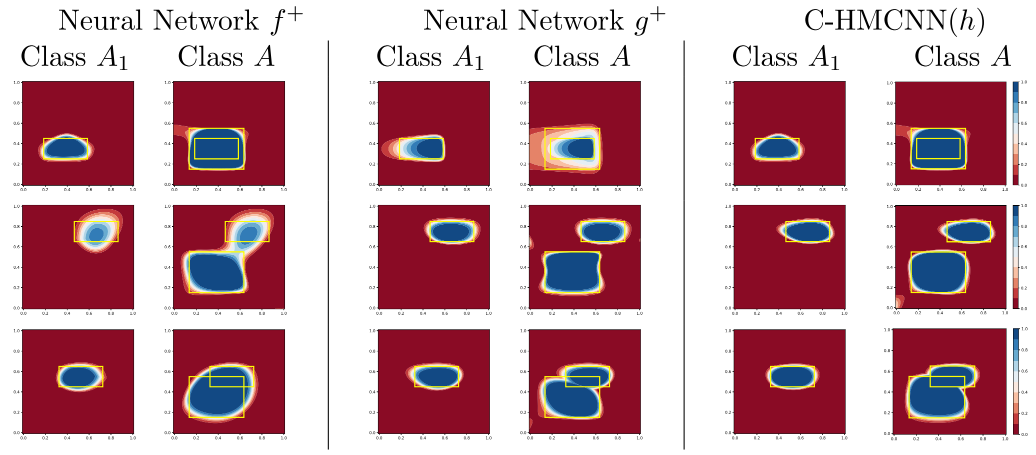

Figure 1: In all figures, the smaller yellow rectangle corresponds to R_1, while the bigger yellow one corresponds to R_2. The first row of figures corresponds to $R_1 \cap R_2 = R_1$, the second corresponds to $R_1 \cap R_2 = \emptyset$, and the third corresponds to $R_1 \cap R_2 \not\in \{R_1, \emptyset\}$. First four columns: decision boundaries of f^+ and g^+ for the classes A_1 and A. Last two columns: decision boundaries of C-HMCNN(h) for the classes A_1 and A. In each figure, the darker the blue (resp., red), the more confident a model is that the data points in the region belong (do not belong) to the class (see the scale at the end of each row).

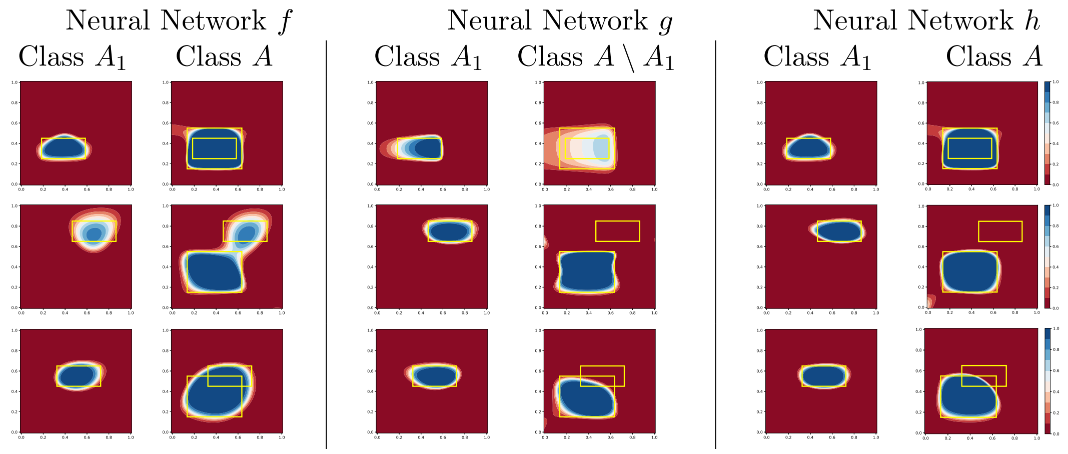

Figure 2: First four columns: decision boundaries of f (resp., g) for the classes A_1 and A (resp., A_1 and $A \setminus A_1$). Last two columns: decision boundaries of h for the classes A_1 and A.

To visualize the problem, assume that $D = 2$, and consider two rectangles R_1 and R_2 with R_1 smaller than R_2, like the two yellow rectangles in the subfigures of Figure 1. Assume $A_1 = R_1$ and $A = R_1 \cup R_2$. Let f^+ be the model obtained by adding a post-processing step to f setting $f^+_{A_1} = \min(f_{A_1}, f_A)$ and $f^+_A = f_A$, as in the works of Cerri et al. (2014, 2016) and Feng et al. (2018) (analogous considerations hold, if we set $f^+_{A_1} = f_{A_1}$ and $f^+_A = \max(f_A, f_{A_1})$ instead). Intuitively, we expect f^+ to perform well even with a very limited number of neurons when $R_1 \cap R_2 = R_1$, as in the first row of Figure 1. However, if $R_1 \cap R_2 = \emptyset$, as in the second row of Figure 1, we expect f^+ to need more neurons to obtain a similar performance. Consider the alternative network g, and let g^+ be the system obtained by setting $g^+_{A_1} = g_{A_1}$ and $g^+_A = \max(g_{A \setminus A_1}, g_{A_1})$. Then, we expect g^+ to perform well when $R_1 \cap R_2 = \emptyset$. However, if $R_1 \cap R_2 = R_1$, we expect g^+ to need more neurons to obtain a similar performance. (We do not consider the model with one output for $A \setminus A_1$ and one for A, since it performs poorly in both cases.) To test our hypothesis, we implemented f and g as feedforward neural networks with one hidden layer with four neurons and *tanh* nonlinearity. We used the *sigmoid* non-linearity for the output layer (from here on, we always assume that the last layer of each neural network presents *sigmoid* non-linearity). f and g were trained with binary cross-entropy loss using Adam optimization (Kingma & Ba, 2015) for 20k epochs with learning rate 10^{-2} ($\beta_1 = 0.9, \beta_2 = 0.999$). The datasets consisted of 5000 (50/50 train/test split) data points sampled from a uniform distribution over $[0, 1]^2$. The first four columns of Figure 1 show the decision boundaries of f^+ and g^+, while the decision boundaries of f and g are reported in Figure 2. These figures highlight that f^+ (resp., g^+) approximates the two rectangles better than g^+ (resp., f^+) when $R_1 \cap R_2 = R_1$ (resp., $R_1 \cap R_2 = \emptyset$). In general, when $R_1 \cap R_2 \notin \{R_1, \emptyset\}$, we expect that the behavior of f^+ and g^+ depends on the relative position of R_1 and R_2.

Ideally, we would like to build a neural network that is able to have roughly the same performance of f^+ when $R_1 \cap R_2 = R_1$, of g^+ when $R_1 \cap R_2 = \emptyset$, and better than both in any other case. We can achieve this behavior in two steps.

In the first step, we build a new neural network consisting of two modules: (i) a bottom module h with two outputs in $[0, 1]$ for A_1 and A, and (ii) an upper module, called *max constraint module* (CM), consisting of a single layer that takes as input the output of the bottom module and imposes the hierarchy constraint. We call the obtained neural network the *coherent hierarchical multi-label classification neural network of h*, denoted C-HMCNN(h). Consider a data point x. Let h_{A_1} and h_A be the outputs of h for the classes A_1 and A, respectively, and let y_{A_1} and y_A be the ground truth for the classes A_1 and A, respectively. The outputs of CM (which are also the output of C-HMCNN(h)) are:

$$\begin{aligned} \mathrm{CM}_{A_1} &= h_{A_1}, \\ \mathrm{CM}_A &= \max(h_A, h_{A_1}). \end{aligned} \tag{5}$$

Notice that the output of C-HMCNN(h) ensures that no hierarchy violation happens, that is, that for any threshold, it cannot be the case that CM predicts that a data point belongs to A_1 but not to A.

In the second step, to exploit the hierarchy constraint during training, C-HMCNN(h) is trained with a novel loss function, called *max constraint loss (*CLoss*)*, defined as CLoss = $\mathrm{CLoss}_{A_1} + \mathrm{CLoss}_A$, where:

$$\begin{aligned} \mathrm{CLoss}_{A_1} &= -y_{A_1} \ln(\mathrm{CM}_{A_1}) - (1 - y_{A_1}) \ln(1 - \mathrm{CM}_{A_1}), \\ \mathrm{CLoss}_A &= -y_A \ln(\max(h_A, h_{A_1} y_{A_1})) - (1 - y_A) \ln(1 - \mathrm{CM}_A)). \end{aligned} \tag{6}$$

CLoss differs from the standard binary cross-entropy loss $\mathcal{L}$:

$$\mathcal{L} = -y_{A_1} \ln(\mathrm{CM}_{A_1}) - (1 - y_{A_1}) \ln(1 - \mathrm{CM}_{A_1}) - y_A \ln(\mathrm{CM}_A) - (1 - y_A) \ln(1 - \mathrm{CM}_A),$$

iff $x \notin A_1$ ($y_{A_1} = 0$), $x \in A$ ($y_A = 1$), and $h_{A_1} > h_A$.

The following example highlights the different behavior of CLoss compared to $\mathcal{L}$.

Example 2.3. Assume $h_{A_1} = 0.3$, $h_A = 0.1$, $y_{A_1} = 0$, and $y_A = 1$. Then,

$$\text{CLoss} = \text{CLoss}_{A_1} + \text{CLoss}_A = -\ln(1 - h_{A_1}) - \ln(h_A)\,,$$

and the partial derivatives of CLoss with respect to h_{A_1} and h_A are

$$\frac{\partial \text{CLoss}}{\partial h_{A_1}} = -\frac{1}{h_{A_1} - 1} \sim 1.4 \qquad \text{and} \qquad \frac{\partial \text{CLoss}}{\partial h_A} = -\frac{1}{h_A} = -10\,,$$

and C-HMCNN(h) rightly learns that it needs to decrease h_{A_1} and increase h_A.

On the other hand, if we use the standard binary cross-entropy $\mathcal{L}$ after CM, we obtain:

$$\mathcal{L} = -\ln(1 - \text{CM}_{A_1}) - \ln(\text{CM}_A) = -\ln(1 - h_{A_1}) - \ln(h_{A_1})\,,$$

and then

$$\frac{\partial \mathcal{L}}{\partial h_{A_1}} = -\frac{1}{h_{A_1} - 1} - \frac{1}{h_{A_1}} \sim -1.9 \qquad \text{and} \qquad \frac{\partial \mathcal{L}}{\partial h_A} = 0\,.$$

Hence, if C-HMCNN(h) is trained with $\mathcal{L}$, then it wrongly learns that it needs to increase h_{A_1} and keep h_A. $\lhd$

Consider the example in Figure 1. To check that our model behaves as expected, we implemented h as f, and trained C-HMCNN(h) with CLoss on the same datasets and in the same way as f and g. The last two columns of Figure 1 show the decision boundaries of C-HMCNN(h), while those of h can be seen in Figure 2. C-HMCNN(h)'s decision boundaries mirror those of f^+ (resp., g^+) when $R_1 \cap R_2 = R_1$ (resp., $R_1 \cap R_2 = \emptyset$). Intuitively, as highlighted by Figure 2, C-HMCNN(h) is able to decide whether to learn A:

1. as a whole (top figure),
2. as the union of $A \setminus A_1$ and A_1 (middle figure), and
3. as the union of a subset of A and a subset of A_1 (bottom figure).

C-HMCNN(h) has thus learned when to exploit the prediction on the lower class A_1 to make predictions on the upper class A. In this case, this happens for

1. 0% of the points in A_1 when $R_1 \cap R_2 = R_1$ as in the top figure,
2. 100% of the points in A_1 when $R_1 \cap R_2 = \emptyset$ as in the middle figure, and
3. 85% of the points in A_1 when R_1 and R_2 are as in the bottom figure.

2.3 General Case

We now consider an arbitrary HMC problem $(\mathcal{P}, \Pi)$ with $\mathcal{P} = (\mathcal{A}, \mathcal{X})$.

Given a class $A \in \mathcal{A}$, we denote by $\mathcal{D}_A$ the set of subclasses of A as given by Π, that is, the set of classes B such that there is a path of length ≥ 0 from B to A in the graph with an edge from A_1 to A for each constraint (4) in Π.

Consider a data point $x \in \mathbb{R}^D$ and a model h for $\mathcal{P}$.

The basic idea is to leverage the predictions on the lower classes to make predictions on the upper classes in the hierarchy. Indeed, for a class A, it may be the case that there exists one subclass $A_1 \in \mathcal{D}_A$ with $h_{A_1} > h_A$: in this case, we want to set $h_A = h_{A_1}$, that is, we want C-HMCNN(h) to delegate the prediction on A to A_1.

Definition 2.4 (Delegate)**.** Let $(\mathcal{P}, \Pi)$ be an HMC problem. Let h be a model for $\mathcal{P}$. Let A and A_1 be two classes with $A_1 \in \mathcal{D}_A$. C-HMCNN(h) *delegates* the prediction on A to A_1 for a data point, if C-HMCNN$(h)_A = h_{A_1}$ and $h_{A_1} > h_A$.

In the general case, we want C-HMCNN(h) to delegate the prediction on A to the subclass A_1 of A having maximum h_{A_1}. This is obtained by defining the output CM_A of C-HMCNN(h) for a class A to be:

$$\text{CM}_A = \max_{B \in \mathcal{D}_A} (h_B). \tag{7}$$

For each class A, the number of operations performed by CM_A is independent from the depth of the hierarchy, making C-HMCNN(h) a scalable model. Thanks to CM, C-HMCNN(h) is guaranteed to always output predictions satisfying the hierarchy constraints, as stated by the following theorem, which follows immediately from Eq. (7).

Theorem 2.5. *Let $(\mathcal{P}, \Pi)$ be an HMC problem. For any model h for $\mathcal{P}$,* C-HMCNN*(h) does not commit any hierarchy violations.*

As an immediate consequence, C-HMCNN(h) also does not commit any logical violations and is coherent relative to the hierarchy constraints.

Corollary 2.6. *Let $(\mathcal{P}, \Pi)$ be an HMC problem. For any model h for $\mathcal{P}$,* C-HMCNN*(h) does not commit any logical violations and is coherent with respect to* Π.

The next step is to improve performance by modifying the loss function in order to exploit the constraints. For each class A, CLoss_A is defined as:

$$\text{CLoss}_A = -y_A \ln(\max_{B \in \mathcal{D}_A} (y_B h_B)) - (1 - y_A) \ln(1 - \text{CM}_A)\,,$$

where y_A is the ground truth class for A. The final CLoss is then given by:

$$\text{CLoss} = \sum_{A \in \mathcal{A}} \text{CLoss}_A. \tag{8}$$

CLoss has the fundamental property that the negative gradient descent algorithm behaves as expected, that is, that for each class, it moves in the “right” direction as given by the ground truth. This is formally expressed by the following theorem.

Theorem 2.7. *Let $(\mathcal{P}, \Pi)$ be an HMC problem. For any model h for $\mathcal{P}$ and class A, let $\frac{\partial \text{CLoss}}{\partial h_A}$ be the partial derivative of* CLoss *with respect to h_A. For each data point, if $y_A = 0$, then $\frac{\partial \text{CLoss}}{\partial h_A} \geq 0$, and if $y_A = 1$, then $\frac{\partial \text{CLoss}}{\partial h_A} \leq 0$.*

Proof. Proof in Appendix C. □

Example 2.3 already pointed out that the standard loss function may not behave as expected. This becomes even more apparent in the general case. Indeed, as highlighted by the following example, the more superclasses a class has, the more likely it is that C-HMCNN(h) trained with the standard binary cross-entropy loss $\mathcal{L}$ will not behave correctly.

Example 2.8. Consider an HMC problem with $n+1$ classes $A, A_1, \dots, A_n$. Assume

1. $A \in \cap_{i=1}^{n} \mathcal{D}_{A_i}$,
2. $h_A > \max(h_{A_1}, \dots, h_{A_n})$, and
3. $y_A = 0$ while $y_{A_1} = \dots = y_{A_n} = 1$.

Then, for the standard binary cross-entropy loss $\mathcal{L}$, we obtain:

$$\mathcal{L} = \mathcal{L}_A + \sum_{i=1}^{n} \mathcal{L}_{A_i}, \qquad \mathcal{L} = -\ln(1-h_A) - n\ln(h_A), \qquad \frac{\partial \mathcal{L}}{\partial h_A} = \frac{1}{1-h_A} - \frac{n}{h_A}.$$

Since $y_A = 0$, we would like to get $\frac{\partial \mathcal{L}_A}{\partial h_A} \geq 0$. However, this is possible only if $h_A \geq \frac{n}{n+1}$: if $n = 1$, then we need $h_A \geq 0.5$, while if $n = 10$, then we need $h_A \geq 10/11 \sim 0.91$. On the other hand, for CLoss, we obtain:

$$\text{CLoss} = \text{CLoss}_A + \sum_{i=1}^{n} \text{CLoss}_{A_i}, \quad \text{CLoss} = -\ln(1-h_A) + \sum_{i=1}^{n} \text{CLoss}_{A_i}, \quad \frac{\partial \text{CLoss}}{\partial h_A} = \frac{1}{1-h_A}.$$

No matter the value of h_A, we get $\frac{\partial \text{CLoss}_A}{\partial h_A} > 0$. $\lhd$

3. Multi-Label Classification with Hard Logical Constraints

In this section, we first introduce logically constrained multi-label classification (LCMC) problems, and then (analogously to what we did in the HMC case) we present the intuitions at the basis of our model CCN(h) through a simple LCMC problem. Thereafter, we finally provide the general solution. We keep the same notation and terminology as introduced in the HMC case.

3.1 Preliminaries

Borrowing notation and concepts from the area of logic programming, we consider *logically constrained multi-label classification* (LCMC) problems, defined as MC problems with a finite set Π of *constraints* or *(normal) rules* r having the form (9):

$$A_1, \dots, A_k, \neg A_{k+1}, \dots, \neg A_n \to A, \qquad (0 \leq k \leq n), \tag{9}$$

where $A, A_1, \dots, A_n$ are classes. We also assume, w.l.o.g., that $A_i \neq A_j$ for $1 \leq i < j \leq k$ and for $k+1 \leq i < j \leq n$. We call $\mathit{head}(r) = A$ the *head* of r, and $\mathit{body}(r) = \mathit{body}^+(r) \cup \mathit{body}^-(r)$ the *body* of r, where $\mathit{body}^+(r) = \{A_1, \dots, A_k\}$ and $\mathit{body}^-(r) = \{\neg A_{k+1}, \dots, \neg A_n\}$. We say that r is *definite* if $n = k$.

Constraint (9) imposes that for each data point x and model m, if m predicts the classes $A_1, \dots, A_k$ and not $A_{k+1}, \dots, A_n$, then m must also predict A. Given this logical interpretation, we can thus define the concepts of logical violation and coherency, which generalize the corresponding definitions given for the hierarchical case.

Definition 3.1. Let $(\mathcal{P}, \Pi)$ be an LCMC problem. Let m be a model for $\mathcal{P}$. If for a data point and a constraint $r \in \Pi$ of the form (9), m predicts $A_1, \dots, A_k$ and not $A_{k+1}, \dots, A_n, A$, then m commits a *logical violation* with respect to r. If m commits no logical violations, then m is *coherent* with respect to Π.

The above definition allows us to determine whether any model m is coherent with respect to the given constraints. However, we want to go beyond coherency and generalize what we did in the HMC setting: whenever convenient, exploit the constraints to compute a value for the classes in the head to ensure coherency and improve performance.

For ease of presentation, assume that we have a single constraint r of the form (9).

In the special case where r is definite ($n = k$), we can associate with the head A a value that is at least the smallest value associated with the classes in the body, that is, we can set

$$m_A = \min(m_{A_1}, \dots, m_{A_k}).$$

In this case, the constraint r is always satisfied for any threshold θ. This corresponds to interpreting (9) according to the Gödel t-norm T_G (Metcalfe, 2005), which is the only function $T : [0,1]^2 \to [0,1]$ that, for every $a, b, c \in [0,1]$, satisfies the following properties (common to all t-norms):

$$\begin{aligned} T(a,b) &= T(b,a), & T(a,1) &= a, \\ T(a,T(b,c)) &= T(T(a,b),c), & T(a,0) &= 0, \\ a \leq b \to T(a,c) &\leq T(b,c), \end{aligned}$$

and also the following (*idempotency*, characterizing T_G):

$$T(a,a) = a.$$

If r is not definite ($n > k$), given $m_{A_{k+1}}, \dots, m_{A_n}$, we need to compute values $\overline{m}_{A_{k+1}}, \dots, \overline{m}_{A_n}$ such that, for each class $A_i \in \{A_{k+1}, \dots, A_n\}$ and threshold θ,

1. $\overline{m}_{A_i} = 1$ when $m_{A_i} = 0$, and $\overline{m}_{A_i} = 0$ when $m_{A_i} = 1$,
2. $\overline{m}_{A_i}$ is strictly decreasing and continuous (small changes to the value of m_{A_i} should correspond to small changes in the value of $\overline{m}_{A_i}$), and
3. $\overline{m}_{A_i} = \theta$ when $m_{A_i} = \theta$.

The first two conditions say that the function $\overline{v}$ of $v \in [0,1]$ is a *strict negation* (Metcalfe, 2005),[1] and, together with the third entail

1. if $m_{A_i} > \theta$, then $\overline{m}_{A_i} < \theta$,
2. if $m_{A_i} < \theta$, then $\overline{m}_{A_i} > \theta$.

1. A negation is non-strict if it is either non-strictly decreasing or non-continuous. An example of a non-strict negation is the residual negation in the Gödel t-norm according to which we would have $\overline{m}_A = 1$ if $m_A = 0$, and $\overline{m}_A = 0$, otherwise.

For any threshold θ there are infinitely many functions $\overline{v}$ satisfying such requirements. A simple solution is to require $\overline{v}$ to be piecewise linear with two segments joining when $\overline{v} = v = \theta$, in which case,

1. $\overline{v}$ is a *strong negation* (Metcalfe, 2005), since $\overline{\overline{v}} = v$, and
2. if $\theta = 0.5$, we obtain $\overline{v} = 1 - v$, that is the *standard negation* in fuzzy logics.

For simplicity, from here on, we assume to have the standard negation, that is, to fix the threshold θ to 0.5 and $\overline{v} = 1 - v$, for each $v \in [0,1]$. All the definitions and results generalize to the case in which we have an arbitrary strict negation with $\overline{\theta} = \theta$.

Given the above, we can now introduce the concept of constraint violation, generalizing the corresponding definition of hierarchy violation.

Definition 3.2. Let $(\mathcal{P}, \Pi)$ be an LCMC problem. Let m be a model for $\mathcal{P}$. If for a data point and for a constraint (9) in Π, m does not satisfy

$$\min(m_{A_1}, \ldots, m_{A_k}, \overline{m}_{A_{k+1}}, \ldots, \overline{m}_{A_n}) \leq m_A, \tag{10}$$

then m commits a *constraint violation*.

The following theorem easily follows from the previous two definitions.

Theorem 3.3. *Let $(\mathcal{P}, \Pi)$ be an LCMC problem. Let m be a model for $\mathcal{P}$. If m does not commit constraint violations, then m is coherent with respect to Π.*

3.2 Basic Case

We now present the main ideas behind our model CCN(h) through a simple LCMC problem. Assume that we have an MC problem with three classes A, A_1, and A_2, and we know that A_1 and A_2 are subsets of A, and that A_2 includes the set of data points belonging to A and not to A_1. Then, $A_1 \cup A_2 \subseteq A$ can be imposed with the constraints

$$A_1 \to A; \qquad A_2 \to A, \tag{11}$$

having the form (4), while $A \setminus A_1 \subseteq A_2$ can be expressed as

$$A, \neg A_1 \to A_2, \tag{12}$$

which imposes, to any model m that, for each $x \in \mathbb{R}^D$, if m predicts A and not A_1, then m must also predict A_2.

Our goal is to develop a method that is able to leverage standard neural network approaches for MC problems, while exploiting all the above constraints in order to produce predictions that are guaranteed to satisfy the constraints while improving performance and extending the method presented for HMC problems.

To understand how the three constraints can be exploited to improve performance, assume that $D = 2$, and consider the yellow (R_1) and green (R_2) rectangles in Figure 3. Assume that $A = R_1 \cup R_2$, $A_1 = R_1$, and $A_2 = R_2 \setminus R_1$. Let f be a neural network with one output for each class to be learned. Intuitively, when R_1 and R_2 are as in the first row of

Figure 3, we can expect to be more difficult for f to learn A than to learn A_1 and A_2. Hence, we would like to exploit the information coming from (11) to learn A, given A_1 and A_2. On the other hand, when the two rectangles are arranged as in the second row, we can expect to be more difficult for f to learn A_2 than A and A_1. In this case, we would like to exploit the information coming from (12) to learn A_2, given A and A_1. Finally, when R_1 and R_2 are arranged as in the third row of the figure, learning both A and A_2 will be difficult, and hence we would like to be able to exploit all the constraints in (11) and (12) to improve performance.

As for C-HMCNN(h), we can achieve our goal in two steps. In the first step, we build a new neural network consisting of two modules: (i) a bottom module h, which can be any neural network with one output for A, A_1, and A_2, respectively, and (ii) an upper *constraint module* (CM), that takes as input the output of the bottom module and imposes the constraints. We call the obtained neural network *coherent-by-construction network* (CCN(h)).

Consider a data point x. Let h_A, h_{A_1}, and h_{A_2} be the outputs of h for the classes A, A_1, and A_2 respectively. Let y_A, y_{A_1}, and y_{A_2} be the ground truth for the classes A, A_1, and A_2, respectively. Let CM_A, CM_{A_1}, and CM_{A_2} be the outputs of CM (which are the outputs of CCN(h)).

We want CCN(h) to extend the set of classes associated with x by the bottom module h, exploiting, and thus satisfying, the constraints. This is obtained by defining CM_A, CM_{A_1}, and CM_{A_2} to be the smallest values such that

$$\begin{aligned}\mathrm{CM}_A &= \max(h_A, \mathrm{CM}_{A_1}, \mathrm{CM}_{A_2}),\\ \mathrm{CM}_{A_1} &= h_{A_1},\\ \mathrm{CM}_{A_2} &= \max(h_{A_2}, \min(\mathrm{CM}_A, \overline{\mathrm{CM}}_{A_1})).\end{aligned} \tag{13}$$

Indeed, the first equation ensures that (i) x will be associated with the class A whenever h already predicts it, and that (ii) CM_{A_1}, $\mathrm{CM}_{A_2} \leq \mathrm{CM}_A$; thus guaranteeing that (11) is satisfied. The other equations have a similar reading. Depending on the values of h_A, h_{A_1}, and h_{A_2}, (13) may admit more than one solution, but we will show (see Example 3.16 and Theorem 3.17) that none of them has a value for CM_A, CM_{A_1}, and CM_{A_2} smaller than that defined by

$$\begin{aligned}\mathrm{CM}_A &= \max(h_A, h_{A_1}, h_{A_2}),\\ \mathrm{CM}_{A_1} &= h_{A_1},\\ \mathrm{CM}_{A_2} &= \max(h_{A_2}, \min(h_A, \overline{h}_{A_1}), \min(h_{A_1}, \overline{h}_{A_1})),\end{aligned}$$

which we define to be the outputs of CM.

In the second step, to effectively exploit the constraints during training, CCN(h) is trained with a new loss function, called *constraint loss* (CLoss), which has two goals:

1. we want to give each class the correct supervision (e.g., if $y_A = 1$, then we want to teach h to increase h_A and not to decrease it), and

2. given a constraint, we want to teach h to rely on the prediction for the classes in the body to make prediction for the class in the head only when the body is satisfied (e.g., for (12), when $y_A = 1$ and $y_{A_1} = 0$).

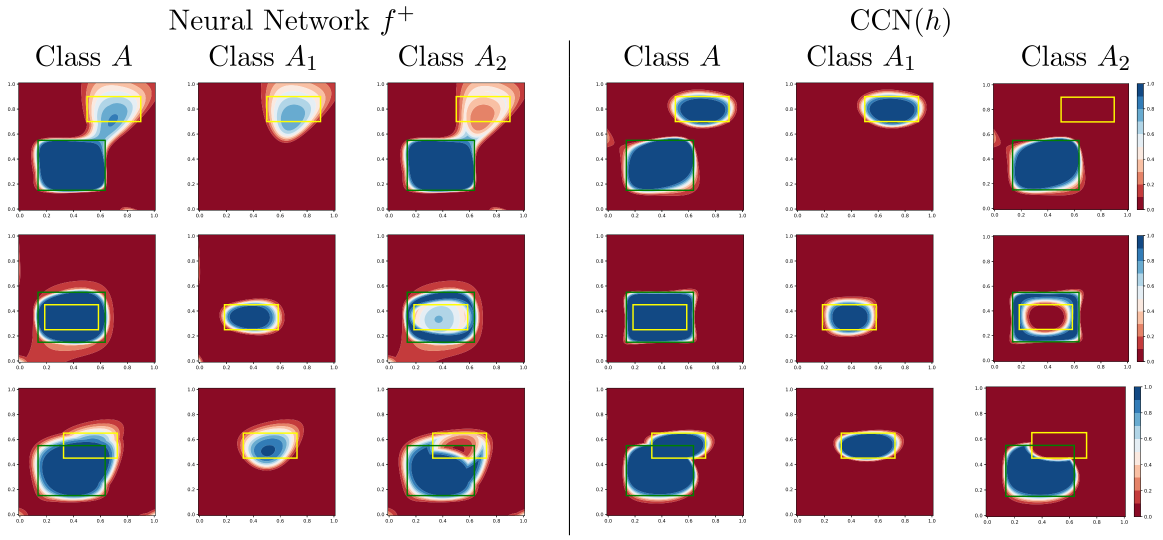

Figure 3: First three columns: decision boundaries of f for the classes A, A_1, and A_2. Last three columns: decision boundaries of CCN(h) for the classes A, A_1, and A_2. In each figure, the darker the blue (resp., red), the more confident a model is that the data points in the region is associated (not associated) with the class (see the scale at the end of each row).

To achieve the above goals, CLoss is defined as $\text{CLoss} = \text{CLoss}_A + \text{CLoss}_{A_1} + \text{CLoss}_{A_2}$, where:

$$\begin{aligned}
\text{CLoss}_A =& - y_A \ln(\max(h_A, h_{A_1} y_{A_1}, h_{A_2} y_{A_2})) - \overline{y}_A \ln(\overline{\text{CM}}_A),\\
\text{CLoss}_{A_1} =& - y_{A_1} \ln(\text{CM}_{A_1}) - \overline{y}_{A_1} \ln(\overline{\text{CM}}_{A_1}),\\
\text{CLoss}_{A_2} =& - y_{A_2} \ln(\max(h_{A_2}, \min(h_A y_A, \overline{h}_{A_1} \overline{y}_{A_1}), \min(h_{A_1} y_{A_1}, \overline{h}_{A_1} \overline{y}_{A_1})))\\
& - \overline{y}_{A_2} \ln(1 - \max(h_{A_2}, \min(h_A \overline{y}_A + y_A, \overline{h}_{A_1} y_{A_1} + \overline{y}_{A_1}), \min(h_{A_1} \overline{y}_{A_1} + y_{A_1}, \overline{h}_{A_1} y_{A_1} + \overline{y}_{A_1}))).
\end{aligned}$$

CLoss differs from the standard binary cross entropy loss function $\mathcal{L}$, as highlighted by the following example.

Example 3.4. Assume that $h_A = 0.6$, $h_{A_1} = 0.2$, $h_{A_2} = 0.3$, $y_A = y_{A_1} = 1$, and $y_{A_2} = 0$. Then,

$$\text{CLoss} = \text{CLoss}_A + \text{CLoss}_{A_1} + \text{CLoss}_{A_2} = -\ln(h_A) - \ln(h_{A_1}) - \ln(h_{A_1}),$$

and

$$\frac{\partial \text{CLoss}}{\partial h_A} = -\frac{1}{h_A} \sim -1.6, \qquad \frac{\partial \text{CLoss}}{\partial h_{A_1}} = -\frac{2}{h_{A_1}} = -10, \qquad \frac{\partial \text{CLoss}}{\partial h_{A_2}} = 0,$$

and CCN(h) rightly learns to increase both h_A and h_{A_1}.

On the other hand, using the standard binary cross-entropy loss $\mathcal{L}$ after CM, we obtain:

$$\mathcal{L} = -\ln(\text{CM}_A) - \ln(\text{CM}_{A_1}) - \ln(\overline{\text{CM}}_{A_2}) = -\ln(h_A) - \ln(h_{A_1}) - \ln(\overline{h}_A),$$

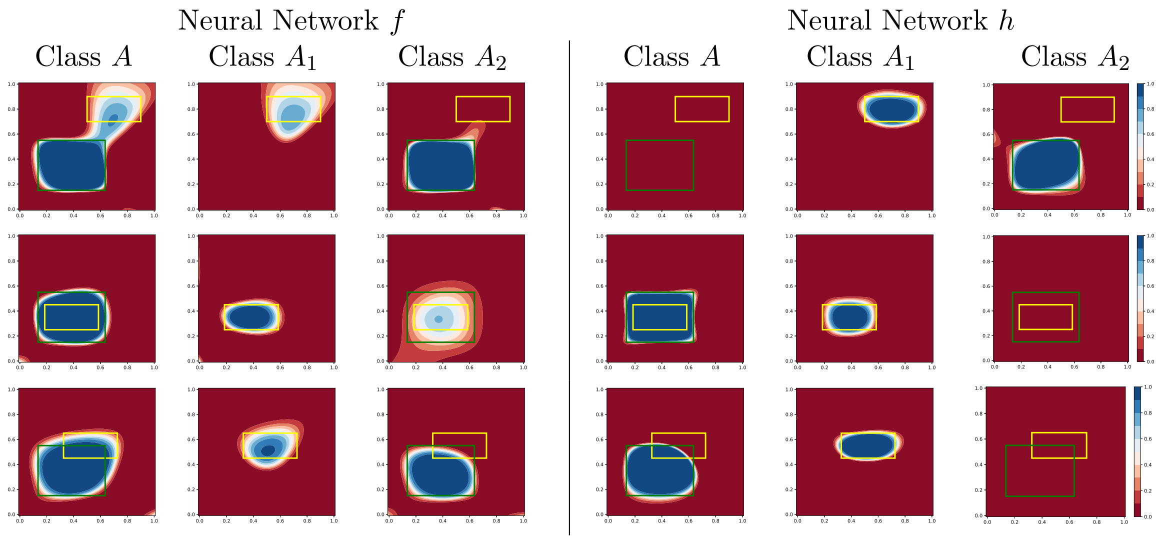

Figure 4: First three columns: decision boundaries of f for the classes A, A_1, and A_2. Last three columns: decision boundaries of CCN(h) for the classes A, A_1, and A_2.

and thus

$$\frac{\partial \mathcal{L}}{\partial h_A} = -\frac{1}{h_A} + \frac{1}{\overline{h}_A} \sim 0.8, \qquad \frac{\partial \mathcal{L}}{\partial h_{A_1}} = -\frac{1}{h_{A_1}} = -5, \qquad \frac{\partial \mathcal{L}}{\partial h_{A_2}} = 0\,.$$

Hence, if trained with $\mathcal{L}$, CCN(h) would learn to decrease h_A while keeping h_{A_2} despite the fact that $y_A = 1$. $\triangleleft$

To test the effectiveness of our approach, we consider again the yellow (R_1) and green (R_2) rectangles in Figure 3 with $A = R_1 \cup R_2$, $A_1 = R_1$, and $A_2 = R_2 \setminus R_1$. We implemented f and h as feedforward neural networks with one hidden layer with 4 neurons and *tanh* nonlinearity. We trained f with binary cross-entropy loss, and CCN(h) using CLoss. We trained both networks for 20k epochs using Adam optimization (Kingma & Ba, 2015), with learning rate 10^{-2} ($\beta_1 = 0.9, \beta_2 = 0.999$). The datasets consisted of 5000 (50/50 train/test split) data points sampled from a uniform distribution over $[0,1]^2$. In order to obtain predictions that are compliant with the constraints also for the neural network f, we apply an additional post-processing step at inference time, obtaining f^+, whose outputs are defined as follows:

$$\begin{aligned} f^+_A &= \max(f_A, f_{A_1}, f_{A_2}), \\ f^+_{A_1} &= f_{A_1}, \\ f^+_{A_2} &= \max(f_{A_2}, \min(f_A, \overline{f}_{A_1}), \min(f_{A_1}, \overline{f}_{A_1})). \end{aligned} \tag{14}$$

We plot the final decision boundaries of f^+ (first three columns) and CCN(h) (last three columns) for all classes in Figure 3, while the decision boundaries of f (first three columns) and h (last three columns) are plotted in Figure 4. In these figures, we can see that f struggles, as expected, in learning the decision boundaries for the classes A and A_2, and that the application of the constraints as a post-processing step, as it happens in f^+, can lead to a decay in performance. On the contrary, we can see that CCN(h) is able to easily learn the decision boundaries for all the classes through a smart exploitation of the constraints. Indeed, as it can be seen in the last three columns of Figure 4, on the ground of the positions of the rectangles R_1 and R_2, CCN(h) knows which constraints to exploit:

- if R_1 and R_2 are arranged as in the first row, then CCN(h) exploits the constraints $A_1 \to A$ and $A_2 \to A$. Thus, the bottom module h does not learn A, which is instead computed from A_1 and A_2,
- if R_1 and R_2 are arranged as in the second row, then CCN(h) exploits the constraint $A, \neg A_1 \to A_2$. Thus, the bottom module h does not learn A_2, which is instead computed from A_1 and A_2, and
- if R_1 and R_2 are arranged as in the third row, then CCN(h) exploits the constraints $A, \neg A_1 \to A_2$ and $A_1 \to A$. Thus, the bottom module h does not learn A_2, and learns A only partially. Then, A_2 is computed from A and A_1, while A exploits A_1 to make predictions on the points belonging to R_2.

3.3 General Case

We now present the general solution. We consider a general LCMC problem $(\mathcal{P}, \Pi)$ and a model h for $\mathcal{P}$. We first show how CCN(h) computes the set of classes associated to every data point (Section 3.3.1), and why the definition of CM requires some care in order to satisfy some desired properties, stated and motivated at the beginning of the same section. We then present the loss function used to train CCN(h) (Section 3.3.2). We end stating that CCN(h) is a generalization of C-HMCNN(h), that is, that C-HMCNN(h) and CCN(h) have the same behavior when given an HMC problem (Section 3.3.3).

3.3.1 Constraint Module — CM

The basic idea of CCN(h) is to

1. have an initial set of classes decided by h, and
2. have all the other classes predicted also on the grounds of the constraints in Π.

In the example in the basic case, h decides $\{A_1\}$: every data point will have or will not have class A_1 depending on the value of h_{A_1}. The decision on the classes $\{A, A_2\}$ takes into account not only h_A, h_{A_2} but also the constraints. In particular, CCN(h) may

1. predict A given the values of h_{A_1} and h_{A_2}, or
2. predict A_2 given the values of h_A and h_{A_1}.

The final set of classes $\mathcal{M}$ predicted by CCN(h) will

1. extend the set of classes $\mathcal{H}$ predicted by h (i.e., $\mathcal{H} \subseteq \mathcal{M}$) and be coherent with Π;
2. be such that any class in $\mathcal{M} \setminus \mathcal{H}$ is in the head of a constraint r in Π, with the chain of rules used to satisfy *body*(r) grounded in $\mathcal{H}$;

3. include only those classes that are either in $\mathcal{H}$ or are forced to be in $\mathcal{M}$ through the explicit use of chains of rules grounded in $\mathcal{H}$;
4. be unique, that is, there will be no other set of classes $\mathcal{M}'$ satisfying the above requirements.

The first requirement is the obvious one: the constraints in Π must be satisfied, and CCN(h) can only derive more classes in the head of the constraints. Whereas the second requirement is formalized by the concept of supportedness as defined in the work by Apt et al. (1988).

Definition 3.5. Let $(\mathcal{P}, \Pi)$ be an LCMC problem. Let h be a model for $\mathcal{P}$. Let $\mathcal{H}$ be the set of classes predicted by h. A set of classes $\mathcal{M}$ is *supported* relative to $\mathcal{H}$ and Π, if for any class $A \in \mathcal{M}$, $A \in \mathcal{H}$, or there exists a constraint $r \in \Pi$ such that $head(r) = A$, $body^+(r) \subseteq \mathcal{M}$, and for each $\neg B \in body^-(r)$, we have $B \notin \mathcal{M}$.

The third requirement is a minimality condition.

Definition 3.6. Let $(\mathcal{P}, \Pi)$ be an LCMC problem. Let h be a model for $\mathcal{P}$. Let $\mathcal{H}$ be the set of classes predicted by h. $\mathcal{M}$ is *minimal* relative to $\mathcal{H}$ and Π, if there exists no set of classes $\mathcal{M}'$ with $\mathcal{H} \subseteq \mathcal{M}' \subset \mathcal{M}$ that is coherent with Π.

The four requirements together ensure that the final predictions made by CCN(h) are coherent with Π and that can be uniquely explained on the grounds of the initial predictions made by h and the constraints in Π.

Intuitively, we could expect that all the above requirements are met if, for each class A, we could define

$$m_A = \max(h_A, m_A^{r_1}, \ldots, m_A^{r_p}), \tag{15}$$

where $r_1, \ldots, r_p$ are all the constraints in Π with head A and, for each such constraint r_i of the form (9),

$$m_A^{r_i} = \min(m_{A_1}, \ldots, m_{A_k}, \overline{m}_{A_{k+1}}, \ldots, \overline{m}_{A_n}).$$

However, in general, the above equations may lead to not uniquely defined values and not minimal predictions because of circular definitions.

Example 3.7. If Π is the set of constraints

$$A_1 \to A_2; \qquad A_2 \to A_1, \tag{16}$$

then, by Equation (15), $m_{A_1} = \max(h_{A_1}, m_{A_2})$ and $m_{A_2} = \max(h_{A_2}, m_{A_1})$, and this allows for infinitely many solutions, unless $h_{A_1} = 1$ or $h_{A_2} = 1$. Furthermore, any solution with $m_{A_1} = m_{A_2} > \theta$ when $h_{A_1} < \theta$ and $h_{A_2} < \theta$ leads to a set of predictions that satisfies the constraints but is not minimal. $\triangleleft$

We will show that such problems, due to circularities involving only positive classes (as the one in the example), can be solved if we consider the minimum of the set of tuples of values satisfying the equations (15): in the case of Example 3.7, the minimum is $m_{A_1} = m_{A_2} = \max(h_{A_1}, h_{A_2})$.[2]

More problems arise when we have circularities involving negated classes.

2. Given a set S of t-tuples of real numbers, $s_1, \ldots, s_t \in S$ is the *minimum of S* if for every $t_1, \ldots, t_t \in S$ and for every $1 \leq i \leq t$, $s_i \leq t_i$. Such a minimum might not exist.

Example 3.8. If Π is the set of constraints

$$\neg A_1 \to A_2; \qquad \neg A_2 \to A_1, \tag{17}$$

then, by Equation (15), $m_{A_1} = \max(h_{A_1}, \overline{m}_{A_2})$ and $m_{A_2} = \max(h_{A_2}, \overline{m}_{A_1})$, and, for example, for $h_{A_1} = h_{A_2} = 0$, it exists no minimum pair of values satisfying the equations. Further, if we set $m_{A_1} = \max(h_{A_1}, \overline{h}_{A_2})$ and $m_{A_2} = \max(h_{A_2}, \overline{h}_{A_1})$, then if for a data point x, we get $h_{A_1} < \theta$ and $h_{A_2} < \theta$, then $m_{A_1} > \theta$ and $m_{A_2} > \theta$, that is, even if h predicts that x belongs to neither A_1 nor A_2, m predicts that x belongs to both A_1 and A_2, and the set of classes $\mathcal{M} = \{A_1, A_2\}$ is not supported relative to $\mathcal{H} = \emptyset$ and the constraints in (17). $\lhd$

To avoid the situation described in the above example, whenever we use the negation on a class, we should refer to an already known value for the class itself. More specifically, first some classes should be computed without the use of negation. Next, some new classes can be computed possibly using the negation of the already computed classes, and this process can be iterated. When this is possible, the set of constraints is stratified (Apt et al., 1988).

There are several equivalent definitions of stratifiedness. Here, we use the one from the work of Apt et al. (1988).

Definition 3.9. A set of constraints Π is *stratified* if there is a partition $\Pi_1, \Pi_2, \ldots, \Pi_s$ of Π, with Π_1 possibly empty, such that, for every $i \in \{1, \ldots, s\}$,

1. for every class $A \in \cup_{r \in \Pi_i} \mathit{body}^+(r)$, all the constraints with head A in Π belong to $\cup_{j=1}^{i} \Pi_j$;

2. for every $\neg A \in \cup_{r \in \Pi_i} \mathit{body}^-(r)$, all the constraints with head A in Π belong to $\cup_{j=1}^{i-1} \Pi_j$.

$\Pi_1, \Pi_2, \ldots, \Pi_s$ is a *stratification* of Π, and each Π_i is a *stratum*.

The check on whether Π is stratified and then the computation of a stratification can be done on the dependency graph of Π (Apt et al., 1988).

Definition 3.10. Let $(\mathcal{P}, \Pi)$ be an LCMC problem. The *dependency graph* G_Π of Π is the directed graph having the set of classes as nodes and with, for each constraint $r \in \Pi$,

1. a positive edge from each class in $\mathit{body}^+(r)$ to $\mathit{head}(r)$,

2. a negative edge from each class A such that $\neg A \in \mathit{body}^-(r)$ to $\mathit{head}(r)$.

The following theorem is from the work by Apt et al. (1988).

Theorem 3.11. *Let $(\mathcal{P}, \Pi)$ be an LCMC problem. Π is stratified iff the dependency graph G_Π of Π contains no cycles with a negative edge.*

As an easy consequence of the above theorem, every set of constraints containing only definite rules (as, e.g., in the HMC case) is stratified. An example with a stratified and with a non-stratified set of constraints, both containing non definite rules, is the following.

Example 3.12. If $\mathcal{A} = \{A, A_1, A_2, A_3, A_4\}$, and Π is the set of constraints in (11), (12), and $A_3 \to A_4$, that is, $\Pi = \{A_1 \to A;\ A_2 \to A;\ A, \neg A_1 \to A_2;\ A_3 \to A_4\}$, then Π is stratified: for example, take $\Pi_1 = \{A_3 \to A_4\}$, and $\Pi_2 = \Pi \setminus \Pi_1$.[3] Any set containing the constraints in (17) is not stratified. $\lhd$

For a stratified set of constraints, there can be many stratifications, as shown by the following example.

Example 3.13 (Ex. 3.12, cont'd)**.** $\Pi'_1 = \{A_3 \to A_4\}$, $\Pi'_2 = \{A_1 \to A\}$, and $\Pi'_3 = \{A_2 \to A;\ A, \neg A_1 \to A_2\}$ is another stratification of the set Π of constraints in Example 3.12. $\lhd$

However, it is well known in the area of logic programming that all the stratifications lead to the same result (Apt et al., 1988). Given this, comparing the two stratifications in Examples 3.12 and 3.13, the latter has two drawbacks:

1. the class A is in the head of constraints belonging to different strata, and
2. it has one more stratum.

Indeed, for each stratum Π_i, we want to compute a value for all the classes in the head of the constraints in Π_i as a single step on GPUs, and thus

1. we would like to have all the constraints with the same head A just in one stratum, so that we can compute a value for A just once, and
2. we would like to have as few strata as possible, to minimize the number of steps.

Thus, assuming Π is stratified,

1. we compute the acyclic component graph (Cormen et al., 2009) of the dependency graph G_Π of Π, that is, the DAG obtained by shrinking each strongly connected component in G_Π into a single vertex (notice that since Π is stratified, negative edges are not involved in any cycle in G_Π),
2. we assign to the classes in each node of the DAG the number 1 plus the maximum number of negative edges connecting a root to the node, and
3. we define:
   (a) $\mathcal{A}_i$ as the set of classes having the number i assigned at the previous step, and
   (b) Π_i as the set of constraints in Π whose head is in $\mathcal{A}_i$.

We call the above procedure CompStrata(Π). Given a stratified set Π of constraints, CompStrata(Π) computes a partition $\mathcal{A}_1, \ldots, \mathcal{A}_s$ of the set $\mathcal{A}$ of classes and also the corresponding stratification $\Pi_1, \ldots, \Pi_s$ of Π with the smallest possible number of strata.

3. This set Π of constraints is an example of a semi-positive set of rules (Apt et al., 1988). A set Π is *semi-positive* if for every head A of a rule in Π, there is not a rule $r \in \Pi$ with $\neg A \in body(r)$. Every set of definite rules is also semi-positive, and every semi-positve set of rules is stratified.

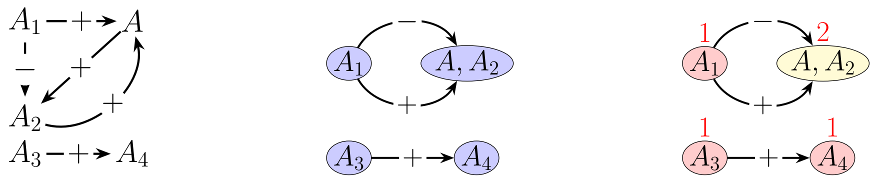

(a) G_Π (b) DAGs from step 1 (c) Numbers from step 2

Figure 5: Given Π as in Example 3.14, visual representation of (a) G_Π, (b) the acyclic component graph of G_Π, (c) the number assigned to each class: 1 to A_1, A_3, A_4, and 2 to A, A_2.

Example 3.14 (Ex. 3.12 cont'd). If $\Pi = \{A_1 \to A;\ A_2 \to A;\ A, \neg A_1 \to A_2;\ A_3 \to A_4\}$, then CompStrata($\Pi$) computes $\mathcal{A}_1 = \{A_1, A_3, A_4\}$, $\mathcal{A}_2 = \{A, A_2\}$, $\Pi_1 = \{A_3 \to A_4\}$, and $\Pi_2 = \Pi \setminus \Pi_1$, as shown in Figure 5. $\lhd$

We now prove that CompStrata(Π) indeed computes the stratification of Π having the smallest number of strata.

Theorem 3.15. *Let $(\mathcal{P}, \Pi)$ be an LCMC problem with stratified Π. Let $\Pi_1, \ldots, \Pi_s$ be the partition of Π computed by* CompStrata(Π)*. Then,*

1. *$\Pi_1, \ldots, \Pi_s$ is a stratification of Π, and*
2. *there exists no stratification of Π with a smaller number of strata.*

Proof. Proof in Appendix D. $\square$

In the sequel, assume Π is stratified, and that $\mathcal{A}_1, \mathcal{A}_2, \ldots, \mathcal{A}_s$ and $\Pi_1, \Pi_2, \ldots, \Pi_s$ are the partition of $\mathcal{A}$ and the stratification of Π computed by CompStrata(Π), respectively.

Consider the ith stratum ($1 \le i \le s$).

If there is more than one stratum ($s > 1$), then we iteratively compute the values for the classes in $\mathcal{A}_i$ $\mathcal{A}_1 \cup \ldots \cup \mathcal{A}_{i-1}$. However, inside each single stratum (even the first one), there can be a chain of rules affecting the values of the classes in the stratum. Consider, for example, the set of constraints $\Pi = \{A_1, A_2 \to A_3; A_3 \to A\}$. In this case,

1. we do not want to first compute the final value for A_3 as $\max(h_{A_3}, \min(h_{A_1}, h_{A_2}))$ and then, in a second step, use it to compute the final value for A (which could be problematic if we also have, e.g., $A \to A_3$), instead
2. we want to directly compute the final value for A as $\max(h_A, h_{A_3}, \min(h_{A_1}, h_{A_2}))$ as a single operation.

We therefore compute and then use the transitive closure of all the constraints in the same stratum. The additional constraints in the closure are conceptually redundant, but they allow for an improvement in performance, as in the work by Deng et al. (2014).

Define Π_i^* to be the set of constraints

1. initially equal to Π_i, and then

2. obtained by recursively adding the constraints obtained from a constraint r already in Π_i^* by substituting a class $A \in \mathit{body}^+(r) \cap \mathcal{A}_i$ with $\mathit{body}(r')$ for any rule r' with $\mathit{head}(r') = A$ (hence, $r' \in \Pi_i$), and finally
3. eliminating the constraints r such that $\mathit{head}(r) \in \mathit{body}^+(r)$, or for which there exists another constraint $r' \in \Pi_i$ with $\mathit{head}(r) = \mathit{head}(r')$ and $\mathit{body}(r') \subset \mathit{body}(r)$.

Π_i^* is guaranteed to be finite, since the set of classes $\mathcal{A}$ is finite, and we do not allow for repetitions in the body of constraints. The constraints being eliminated in the third step are redundant.

Then, for each class $A \in \mathcal{A}_i$, we define the output CM_A of the constraint module CM via

$$\mathrm{CM}_A = \max(h_A, h_A^{r_1}, \ldots, h_A^{r_p}), \tag{18}$$

where

1. $r_1, \ldots, r_p$ are all the constraints in Π_i^* with head A, and
2. assuming $r \in \Pi_i^*$ has the form (9),

$$h_A^r = \min(v_{A_1}, \ldots, v_{A_k}, \overline{\mathrm{CM}}_{A_{k+1}}, \ldots, \overline{\mathrm{CM}}_{A_n}),$$

with $v_{A_1} = h_{A_1}$ if $A_1 \in \mathcal{A}_i$, and $v_{A_1} = \mathrm{CM}_{A_1}$ if $A_1 \in \cup_{j=1}^{i-1} \mathcal{A}_j$. Analogously for $v_{A_2}, \ldots, v_{A_k}$.

The above definition is well-founded:

1. Π_1^* does not contain negated classes, and thus the definition of CM_A when $A \in \mathcal{A}_1$ relies only on the outputs of the bottom module h, and
2. the definition of CM_A when $A \in \mathcal{A}_i$ ($i > 1$) uses only outputs of h or of already defined outputs of CM.

Example 3.16 (Ex. 3.14, cont'd)**.** $\Pi_1 = \Pi_1^* = \{A_3 \to A_4\}$, while $\Pi_2^* = \Pi_2 \cup \{A_1, \neg A_1 \to A_2\}$. Thus,

$$\mathrm{CM}_{A_1} = h_{A_1}, \quad \mathrm{CM}_{A_3} = h_{A_3}, \quad \mathrm{CM}_{A_4} = \max(h_{A_3}, h_{A_4}),$$
$$\mathrm{CM}_A = \max(h_A, \mathrm{CM}_{A_1}, h_{A_2}), \qquad \mathrm{CM}_{A_2} = \max(h_{A_2}, \min(h_A, \overline{\mathrm{CM}}_{A_1}), \min(\mathrm{CM}_{A_1}, \overline{\mathrm{CM}}_{A_1})).$$

If $h_{A_1} = 0.2$, $h_{A_2} = 0.3$, $h_A = 0.6$ (as in Example 3.4), then $\mathrm{CM}_{A_1} = 0.2$, $\mathrm{CM}_{A_2} = 0.6$, $\mathrm{CM}_A = 0.6$.

The constraint $A_1, \neg A_1 \to A_2 \in \Pi_2^*$, which leads to the inclusion of $\min(\mathrm{CM}_{A_1}, \overline{\mathrm{CM}}_{A_1}) = \min(h_{A_1}, \overline{h}_{A_1})$ in the definition of CM_{A_2}, is necessary in order to guarantee that CM never violates (12), that is, that it always holds

$$\min(\mathrm{CM}_A, \overline{\mathrm{CM}}_{A_1}) \leq \mathrm{CM}_{A_2}. \tag{19}$$

Indeed assume, $h_A = h_{A_2} = 0.3, h_{A_1} = 0.6$. Then, $\mathrm{CM}_A = \mathrm{CM}_{A_1} = 0.6$, $\mathrm{CM}_{A_2} = 0.4$, and (19) is satisfied. If we would have defined $\mathrm{CM}_{A_2} = \max(h_{A_2}, \min(h_A, \overline{\mathrm{CM}}_{A_1}))$ (omitting $\min(\mathrm{CM}_{A_1}, \overline{\mathrm{CM}}_{A_1})$), then we would have obtained $\mathrm{CM}_{A_2} = 0.3$, and (19) would have been no longer satisfied. ◁

Given a stratified set Π of constraints, $\mathrm{CCN}(h)$ is guaranteed to always satisfy Π.

Theorem 3.17. *Let $(\mathcal{P}, \Pi)$ be an LCMC problem. Assume Π is stratified. Let h be a model for $\mathcal{P}$. Then, $\mathrm{CCN}(h)$ satisfies Equation (15) and thus commits no constraint violations.*

Proof. Proof in Appendix E. □

Given the values for the classes in $\cup_{j=1}^{i-1}\mathcal{A}_j$, the values of $\mathrm{CCN}(h)$ for the classes in $\mathcal{A}_i$ correspond to the minimum of the set of tuples satisfying (15).

Theorem 3.18. *Let $(\mathcal{P}, \Pi)$ be an LCMC problem. Assume Π is stratified. Let h be a model for $\mathcal{P}$. Let $\mathcal{A}_1, \ldots, \mathcal{A}_s$ be the partition of $\mathcal{A}$ computed by* CompStrata(Π). *For $1 \leq i \leq s$, let m be a model for $\mathcal{P}$ satisfying Equation (15) and such that for every class $B \in \cup_{j=1}^{i-1}\mathcal{A}_j$, $m_B = \mathrm{CCN}(h)_B$. For every class $A \in \mathcal{A}_i$, $m_A \geq \mathrm{CCN}(h)_A$.*

Proof. Proof in Appendix F. □

We can now state that $\mathrm{CCN}(h)$ has the desired properties mentioned at the beginning of the section.

Theorem 3.19. *Let $(\mathcal{P}, \Pi)$ be an LCMC problem. Assume Π is stratified. Let h be a model for $\mathcal{P}$. Let $\mathcal{H}$ be the set of classes predicted by h. Let $\mathcal{M}$ be the set of classes predicted by $\mathrm{CCN}(h)$. Then, $\mathcal{M}$*

1. *extends $\mathcal{H}$ and is coherent with Π,*
2. *is supported relative to $\mathcal{H}$ and Π,*
3. *is minimal relative to $\mathcal{H}$ and Π, and*
4. *is the unique set satisfying the previous properties.*

Proof. Proof in Appendix G. □

If we interpret the given set of constraints as a stratified normal logic program, we can establish a relation with the canonical model semantics of stratified normal logic programs (Apt et al., 1988), which coincides with the stable model semantics (Gelfond & Lifschitz, 1988).

Definition 3.20. Let Π be a finite set of normal rules. Let $\mathcal{M}$ be a set of classes. The *reduct* of Π relative to $\mathcal{M}$ is the set $\Pi^{\mathcal{M}}$ of definite rules obtained by:

1. dropping the rules r in Π such that for a class $A \in \mathcal{M}$, $\neg A \in \mathit{body}(r)$, and then
2. dropping $\mathit{body}^{-}(r)$ from the remaining rules r.

$\mathcal{M}$ is a *stable model* of Π iff $\mathcal{M}$ is the smallest set closed under $\Pi^{\mathcal{M}}$.

Example 3.21. Let $\Pi = \{A_1 \to A;\ A_2 \to A;\ A, \neg A_1 \to A_2;\ A_3 \to A_4\}$. Then,

1. the stable model of Π is the empty set,
2. the stable model of $\Pi \cup \{\to A\}$ is $\{A_2, A\}$, and

3. the stable model of $\Pi \cup \{\to A; \to A_4\}$ is $\{A_2, A_4, A\}$. $\lhd$

Theorem 3.22. *Let $(\mathcal{P}, \Pi)$ be an LCMC problem with stratified Π. Let h be a model for $\mathcal{P}$. Let $\mathcal{H}$ be the set of classes predicted by h. Let $\mathcal{M}$ be the set of classes predicted by* $\text{CCN}(h)$. *Then, $\mathcal{M}$ is the stable model of the set of constraints $\Pi \cup \{\to A : A \in \mathcal{H}\}$.*

Proof. Proof in Appendix H. $\square$

Finally, the definition of the output CM_A of $\text{CCN}(h)$ for class $A \in \mathcal{A}_i$ is based on the computation of Π_i^*, which, as we have seen in Example 3.16, may contain constraints with logically contradictory bodies (i.e., with B and $\neg B$ in the body, for some class B). Indeed, if in the construction of Π_i^* we would have not included such constraints with contradictory bodies, the resulting system may exhibit

1. constraint violations (as seen in Example 3.16), but
2. still no logical violations, since the set of predicted classes does not change.

3.3.2 Constraint Loss — CLoss

In the general case, for every data point, the value of the loss function CLoss used to train $\text{CCN}(h)$ is defined as:

$$\text{CLoss} = \sum_{A \in \mathcal{A}} \text{CLoss}_A,$$

CLoss_A being the value of the loss for class A, defined as:

$$\text{CLoss}_A = -y_A \ln(\text{CM}_A^+) - \overline{y}_A \ln(\overline{\text{CM}_A^-}),$$

where:

- y_A is the ground truth for class A,
- CM_A^+ is the value to optimize when $y_A = 1$, and
- CM_A^- is the value to optimize when $y_A = 0$.

CM_A^+ and CM_A^- differ from the output value CM_A of $\text{CCN}(h)$ for class A, that is, from $\text{CCN}(h)_A$. Indeed, as it has been the case in the HMC setting and already discussed in the basic case, for CM_A^+ and CM_A^- we have to take into account also the ground-truth.

Similarly to what has been done for computing CM_A, for a stratified set of constraints, the computation of CM_A^+ and CM_A^- will be done stratum after stratum, starting from the first. We thus assume:

1. that Π is stratified,
2. that $\mathcal{A}_1, \mathcal{A}_2, \ldots, \mathcal{A}_s$ and $\Pi_1, \Pi_2, \ldots, \Pi_s$ ($s \geq 1$) are the partitions of $\mathcal{A}$ and Π computed by CompStrata(Π), and
3. that $\Pi_1^*, \Pi_2^*, \ldots, \Pi_s^*$ are the sets of constraints corresponding to $\Pi_1, \Pi_2, \ldots, \Pi_s$ and defined as in the previous subsection.

The values CM^+_A and CM^-_A associated to a class A in the ith stratum will depend on the set Π^*_A of constraints with head A in Π^*_i, and thus on:

1. the values computed by model h for A and for the classes in the ith stratum and in the body of a constraint in Π^*_A,
2. the values of the already computed loss for the classes in the lower strata and in the body of a constraint in Π^*_A,
3. the ground truth for the classes in the body of the constraints in Π^*_A.

Consider a class A in the ith stratum (i.e., $A \in \mathcal{A}_i$). To each constraint r with head A in Π^*_i we associate two values

1. $h^{+,r}_A$ to be used with $y_A = 1$, and
2. $h^{-,r}_A$ to be used with $y_A = 0$.

Assume $y_A = 1$. Consider a constraint r in Π^*_i with head A of the form (9). Then, we want to teach CCN(h) to possibly exploit the constraint r for predicting A if $y_{A_1} = \ldots = y_{A_k} = 1$ and $y_{A_{k+1}} = \ldots = y_{A_n} = 0$. We thus define,

$$h^{+,r}_A = \min(v_{A_1} y_{A_1}, \ldots, v_{A_k} y_{A_k}, \overline{v}_{A_{k+1}} \overline{y}_{A_{k+1}}, \ldots, \overline{v}_{A_n} \overline{y}_{A_n}),$$

where v_{A_l} is

1. h_{A_l} if $A_l \in \mathcal{A}_i$ (and thus $1 \leq l \leq k$),
2. $\mathrm{CM}^+_{A_l}$ if $A_l \in \cup_{j=1}^{i-1} \mathcal{A}_j$ and $1 \leq l \leq k$,
3. $\mathrm{CM}^-_{A_l}$ if $A_l \in \cup_{j=1}^{i-1} \mathcal{A}_j$ and $k+1 \leq l \leq n$.

The value CM^+_A associated to class A when $y_A = 1$ is

$$\mathrm{CM}^+_A = \max(h_A, h^{+,r_1}_A, \ldots, h^{+,r_p}_A),$$

where $r_1, \ldots, r_p$ are all the constraints in Π^*_i with head A.

Assume $y_A = 0$. Consider a constraint r in Π^*_i with head A of the form (9). Then, for some class $A_l \in \mathit{body}^+(r)$ $y_{A_l} = 0$, or for some class $A_l \in \mathit{body}^-(r)$ $y_{A_l} = 1$, and we want to teach CCN(h) to not fire the constraint r. We thus define

$$h^{-,r}_A = \min(v_{A_1} \overline{y}_{A_1} + y_{A_1}, \ldots, v_{A_k} \overline{y}_{A_k} + y_{A_k}, \overline{v}_{A_{k+1}} y_{A_{k+1}} + \overline{y}_{A_{k+1}}, \ldots, \overline{v}_{A_n} y_{A_n} + \overline{y}_{A_n}),$$

where v_{A_l} now is

1. h_{A_l} if $A_l \in \mathcal{A}_i$ (and thus $1 \leq l \leq k$),
2. $\mathrm{CM}^-_{A_l}$ if $A_l \in \cup_{j=1}^{i-1} \mathcal{A}_j$ and $1 \leq l \leq k$,
3. $\mathrm{CM}^+_{A_l}$ if $A_l \in \cup_{j=1}^{i-1} \mathcal{A}_j$ and $k+1 \leq l \leq n$.

The value CM_A^- associated with the class A when $y_A = 0$ is

$$\mathrm{CM}_A^- = \max(h_A, h_A^{-,r_1}, \dots, h_A^{-,r_p}),$$

where $r_1, \dots, r_p$ are all the constraints in Π_i^* with head A.

Example 3.23. Consider the simpler version of Example 3.16 with $\mathcal{A} = \{A_1, A_2, A\}$, $\Pi = \{A_1 \to A; A_2 \to A; A, \neg A_1 \to A_2\}$, $h_{A_1} = 0.2$, $h_{A_2} = 0.3$, $h_A = 0.6$, as in Example 3.4. Then, $\mathcal{A}_1 = \{A_1\}$, $\mathcal{A}_2 = \{A, A_2\}$, $\Pi_1^* = \emptyset$, $\Pi_2^* = \Pi \cup \{A_1, \neg A_1 \to A_2\}$ (see also Example 3.16). Assume $y_{A_1} = y_A = 1$ and $y_{A_2} = 0$.

If $r_1, \dots, r_4$ are the constraints listed as above, then

1. $h_A^{+,r_1} = h_{A_1} = 0.2$, $h_A^{+,r_2} = 0$,
2. $\mathrm{CM}_{A_1}^+ = h_{A_1} = 0.2$, $\mathrm{CM}_A^+ = h_A = 0.6$,
3. $h_{A_2}^{-,r_3} = 1 - h_{A_1} = 0.8$, $h_{A_2}^{-,r_4} = 1 - h_{A_1} = 0.8$, and
4. $\mathrm{CM}_{A_2}^- = 1 - h_{A_1} = 0.8$.

Thus,

$$\mathrm{CLoss} = -\ln(h_{A_1}) - \ln(1 - (1 - h_{A_1})) - \ln(h_A) = -2\ln(h_{A_1}) - \ln(h_A),$$

as already calculated in Example 3.4. ◁

As in the hierarchical case, CLoss has the fundamental property that the negative gradient descent algorithm behaves as expected, that is, that for each class, it moves in the "right" direction as given by the ground truth.

Theorem 3.24. *Let $(\mathcal{P}, \Pi)$ be an LCMC problem. For any model h for $\mathcal{P}$ and class A, let $\frac{\partial \mathrm{CLoss}}{\partial h_A}$ be the partial derivative of* CLoss *with respect to h_A. For each data point, if $y_A = 0$, then $\frac{\partial \mathrm{CLoss}}{\partial h_A} \geq 0$, and if $y_A = 1$, then $\frac{\partial \mathrm{CLoss}}{\partial h_A} \leq 0$.*

Proof. Proof in Appendix I. □

3.3.3 Relation Between C-HMCNN(h) and CCN(h)

From the definitions of CM_A and CLoss_A, it is clear that they generalize the corresponding definitions given in the hierarchical case. Thus, C-HMCNN(h) and CCN(h) have the same behavior when considering HMC problems.

Theorem 3.25. *Let $(\mathcal{P}, \Pi)$ be an HMC problem. Let h be a model for $\mathcal{P}$. For any class A,* C-HMCNN*(h)*$_A$ = CCN*(h)*$_A$.

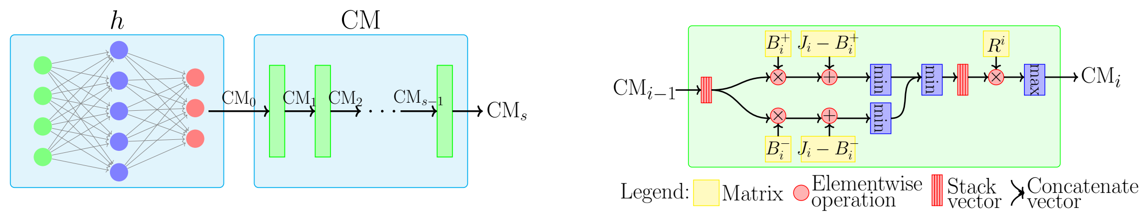

Figure 6: Visual representation of CCN(h) (left), and details of the operations associated with each stratum (right).

4. GPU Implementation

In the previous section, both CM$_A$ and CLoss$_A$ have been defined for a specific class A. However, it is possible to compute both CM$_A$ and CLoss$_A$ for all classes in the same stratum in parallel, leveraging GPU architectures. In this section, we show how to compute the values first of the constraint module and then of the loss function on a GPU. At the end, we show how this computation can be simplified in the HMC case.

Consider an LCMC problem $(\mathcal{P}, \Pi)$ with stratified Π. We assume to have l classes (i.e., $|\mathcal{A}| = l$), that $\Pi_1, \Pi_2, \dots, \Pi_s$ is the stratification computed by CompStrata(Π), and that $\Pi_1^*, \Pi_2^*, \dots, \Pi_s^*$ are the corresponding sets as defined in the previous section.

4.1 Constraint Module

The basic idea, starting from the vector CM$_0$ (which contains the l values resulting from the bottom module h) is to iteratively compute the vector of values CM$_i$ corresponding to the outputs of CM if given the set of constraints $\cup_{j=1}^{i} \Pi_j^*$. The final output of CM will correspond to CM$_s$. Figure 6 shows a visual representation of the process and of CCN(h).

For each $i \in \{1, \dots, s\}$, p_i is the number of constraints in Π_i^* ($p_i = |\Pi_i^*|$), r_{ij} denotes the jth constraint in Π_i^*, and

- B_i^+ is the $p_i \times l$ matrix whose j, k element is 1 if $A_k \in \mathit{body}^+(r_{ij})$, and 0 otherwise;
- B_i^- is the $p_i \times l$ matrix whose j, k element is 1 if $\neg A_k \in \mathit{body}^-(r_{ij})$, and 0 otherwise;
- C_{i-1} is the $p_i \times l$ matrix obtained by stacking p_i times CM$_{i-1}$.

Stacking p times a vector v of size q returns the $p \times q$ matrix $1_p^T \times v$ whose j, k element is $v[k]$.

Then, the jth value $v_i[j]$ of the vector v_i associated with the body of the constraint r_{ij} is

$$v_i^+ = \min(B_i^+ \odot C_{i-1} + (J_{p_i,l} - B_i^+), \dim = 1),$$
$$v_i^- = \min(B_i^- \odot (J_{p_i,l} - C_{i-1}) + (J_{p_i,l} - B_i^-), \dim = 1),$$
$$v_i[j] = \min(v_i^+[j], v_i^-[j]),$$

where

1. $\odot$ represents the Hadamard product,
2. $J_{p,q}$ is the $p \times q$ matrix of ones, and

3. given an arbitrary $p \times q$ matrix Q, $\min(Q, \dim = 1)$ (resp., $\max(Q, \dim = 1)$) returns a vector of length p whose ith element is equal to $\min(Q_{i1}, \dots, Q_{iq})$ (resp., $\max(Q_{i1}, \dots, Q_{iq})$).

Then, the output of the ith layer associated with the ith stratum is given by:

$$\mathrm{CM}_i = \max(IH_i \odot V_i, \dim = 1),$$

where

- H_i is the $l \times p_i$ matrix whose j, k element is 1 if $A_j = head(r_{ik})$, and 0 otherwise,
- IH_i is the $l \times (l + p_i)$ matrix obtained by stacking the $l \times l$ identity matrix and H_i,
- V_i is the $l \times (l + p_i)$ matrix obtained by stacking l times the concatenation of CM_{i-1} and v_i.

Example 4.1. Let $\mathcal{A} = \{A_1, A_2, A\}$, $\Pi = \{A_1 \to A; A_2 \to A; A, \neg A_1 \to A_2\}$, $h_{A_1} = 0.2$, $h_{A_2} = 0.3$, $h_A = 0.6$, as in Example 3.16. Then, $\mathcal{A}_1 = \{A_1\}$, $\mathcal{A}_2 = \{A, A_2\}$, $\Pi_1^* = \emptyset$, $\Pi_2^* = \Pi \cup \{A_1, \neg A_1 \to A_2\}$.

Then, $\mathrm{CM}_0 = \begin{bmatrix} 0.2 & 0.3 & 0.6 \end{bmatrix}$, B_1^+, B_1^-, C_0, H_1 are the empty matrices, IH_1 is the 3×3 identity matrix, while

$$B_2^+ = \begin{bmatrix} 1 & 0 & 0 \\ 0 & 1 & 0 \\ 0 & 0 & 1 \\ 1 & 0 & 0 \end{bmatrix} \quad B_2^- = \begin{bmatrix} 0 & 0 & 0 \\ 0 & 0 & 0 \\ 1 & 0 & 0 \\ 1 & 0 & 0 \end{bmatrix} \quad C_1 = 1_4^T \times \begin{bmatrix} 0.2 & 0.3 & 0.6 \end{bmatrix} = \begin{bmatrix} 0.2 & 0.3 & 0.6 \\ 0.2 & 0.3 & 0.6 \\ 0.2 & 0.3 & 0.6 \\ 0.2 & 0.3 & 0.6 \end{bmatrix}$$

$$H_2 = \begin{bmatrix} 0 & 0 & 0 & 0 \\ 0 & 0 & 1 & 1 \\ 1 & 1 & 0 & 0 \end{bmatrix} \quad IH_2 = \begin{bmatrix} 1 & 0 & 0 & 0 & 0 & 0 & 0 \\ 0 & 1 & 0 & 0 & 0 & 1 & 1 \\ 0 & 0 & 1 & 1 & 1 & 0 & 0 \end{bmatrix}$$

$$V_1 = 1_3^T \times \begin{bmatrix} 0.2 & 0.3 & 0.6 \end{bmatrix} \quad \mathrm{CM}_1 = \begin{bmatrix} 0.2 & 0.3 & 0.6 \end{bmatrix}$$

$$v_2^+ = \begin{bmatrix} 0.2 & 0.3 & 0.6 & 0.2 \end{bmatrix} \quad v_2^- = \begin{bmatrix} 1 & 1 & 0.8 & 0.8 \end{bmatrix} \quad v_2 = v_2^+$$

$$V_2 = 1_3^T \times \begin{bmatrix} 0.2 & 0.3 & 0.6 & 0.2 & 0.3 & 0.6 & 0.2 \end{bmatrix} \quad \mathrm{CM}_2 = \begin{bmatrix} 0.2 & 0.6 & 0.6 \end{bmatrix}$$

and thus $\mathrm{CM}_{A_1} = h_{A_1} = 0.2$, $\mathrm{CM}_{A_2} = h_A = 0.6$, and $\mathrm{CM}_A = h_A = 0.6$, as expected (see Example 3.16). $\lhd$

4.2 Constraint Loss

We now show how to compute CLoss_A for all classes in parallel, leveraging GPU architectures. Here, we define Y_i the $p_i \times l$ matrix obtained by stacking p_i times the ground-truth vector y, and $v_i^+[j]$ to be the value associated with the body of the jth constraint $r_{ij} \in \Pi_i^*$ when the ground-truth class $y_{head(r_{ij})} = 1$:

$$\begin{aligned} v_i^{+\backslash+} &= \min(B_i^+ \odot C_{i-1} \odot Y_i + (J_{p_i,l} - B_i^+), \dim = 1), \\ v_i^{+\backslash-} &= \min(B_i^- \odot (J_{p_i,l} - C_{i-1}) \odot (J_{p_i,l} - Y_i) + (J_{p_i,l} - B_i^-), \dim = 1), \\ v_i^+[j] &= \min(v_i^{+\backslash+}[j], v_i^{+\backslash-}[j]). \end{aligned}$$

Analogously, $v_i^-[j]$ is the value associated with the body of the jth constraint $r_{ij} \in \Pi_i^*$ when $y_{head(r_{ij})} = 0$:

$$\begin{aligned} v_i^{-\backslash+} &= \min(B_i^+ \odot C_{i-1} \odot (J_{p_i,l} - Y_i) + (J_{p_i,l} - B_i^+) + B_i^+ \odot Y_i, \dim = 1), \\ v_i^{-\backslash-} &= \min(B_i^- \odot (J_{p_i,l} - C_{i-1}) \odot Y_i + (J_{p_i,l} - B_i^-) + B_i^- \odot (J_{p_i,l} - Y_i), \dim = 1), \\ v_i^-[j] &= \min(v_i^{-\backslash+}[j], v_i^{-\backslash-}[j]). \end{aligned}$$

Then, the output of the ith layer associated with the ith stratum is given by:

$$\mathrm{CM}_i^{+\backslash-} = \max\big((IH_i \odot V_i^+) \odot IY_i + (IH_i \odot V_i^-) \odot (J_{l,l+p_i} - IY_i), \dim = 1\big),$$

where:

- $\mathrm{CM}_0^{+\backslash-} = \mathrm{CM}_0$,
- IY_i is the $l \times (l + p_i)$ matrix obtained by stacking the $l \times l$ identity matrix and Y_i^T, the transposed of Y_i,
- V_i^+ is the $l \times (l+p_i)$ matrix obtained by stacking l times the concatenation of $\mathrm{CM}_{i-1}^{+\backslash-}$ and v_i^+, and
- V_i^- is the $l \times (l+p_i)$ matrix obtained by stacking l times the concatenation of $\mathrm{CM}_{i-1}^{+\backslash-}$ and v_i^-.

Once we have computed $\mathrm{CM}_s^{+\backslash-}$, we can compute CLoss by using the standard binary cross-entropy loss (BCELoss), as given in any standard library (e.g., PyTorch):

$$\mathrm{CLoss} = \mathrm{BCELoss}(y, \mathrm{CM}_s^{+\backslash-}).$$

Example 4.2 (Ex. 4.1, cont'd)**.** Assume that $y_A = y_{A_1} = 1$, and $y_{A_2} = 0$. Then, $y = \begin{bmatrix}1 & 0 & 1\end{bmatrix}$, Y_1 is the empty matrix, $V_1^+ = V_1^- = V_1$, IY_1 is the identity matrix,

$$\mathrm{CM}_1^{+\backslash-} = \begin{bmatrix}0.2 & 0.3 & 0.6\end{bmatrix}$$

$$B_2^+ \odot C_1 \odot Y_2 + (J_{4,3} - B_2^+) = \begin{bmatrix}0.2 & 1 & 1 \\ 1 & 0 & 1 \\ 1 & 1 & 0.6 \\ 0.2 & 1 & 1\end{bmatrix}$$

$$B_2^- \odot (J_{4,3} - C_1) \odot (J_{4,3} - Y_2) + (J_{4,3} - B_2^-) = \begin{bmatrix} 1 & 1 & 1 \\ 1 & 1 & 1 \\ 0 & 1 & 1 \\ 0 & 1 & 1 \end{bmatrix}$$

$$v_2^+ = \begin{bmatrix} 0.2 & 0 & 0 & 0 \end{bmatrix}$$

The only value which is not 0 is the first one, corresponding to the first constraint, being the only constraint whose body is satisfied by the ground truth.

$$B_2^+ \odot C_1 \odot (J_{4,3} - Y_2) + (J_{4,3} - B_2^+) + B_2^+ \odot Y_2 = \begin{bmatrix} 1 & 1 & 1 \\ 1 & 0.3 & 1 \\ 1 & 1 & 1 \\ 1 & 1 & 1 \end{bmatrix}$$

$$B_2^- \odot (J_{4,3} - C_1) \odot Y_2 + (J_{4,3} - B_2^-) + B_2^- \odot (J_{4,3} - Y_2) = \begin{bmatrix} 1 & 1 & 1 \\ 1 & 1 & 1 \\ 0.8 & 1 & 1 \\ 0.8 & 1 & 1 \end{bmatrix}$$

$$v_2^- = \begin{bmatrix} 1 & 0.3 & 0.8 & 0.8 \end{bmatrix}$$

The values which are not 1 correspond to the last four constraints, being the constraints whose body is not satisfied by the ground truth.

$$Y_2 = 1_4^T \times \begin{bmatrix} 1 & 0 & 1 \end{bmatrix}$$

$$V_2^+ = 1_3^T \times \begin{bmatrix} 0.2 & 0.3 & 0.6 & 0.2 & 0 & 0 & 0 \end{bmatrix} \qquad V_2^- = 1_3^T \times \begin{bmatrix} 0.2 & 0.3 & 0.6 & 1 & 0.3 & 0.8 & 0.8 \end{bmatrix}$$

$$\begin{array}{c} (IH_2 \odot V_2^+) \odot IY_2 \\ + \\ (IH_2 \odot V_2^-) \odot (J_{3,7} - IY_2) \end{array} = \begin{bmatrix} 0.2 & 0 & 0 & 0 & 0 & 0 & 0 \\ 0 & 0.3 & 0 & 0 & 0 & 0.8 & 0.8 \\ 0 & 0 & 0.6 & 0.2 & 0 & 0 & 0 \end{bmatrix}$$

$$\mathrm{CM}_2^{+\backslash -} = \begin{bmatrix} 0.2 & 0.8 & 0.6 \end{bmatrix}$$

The three values of $\mathrm{CM}_2^{+\backslash -}$ correspond to the expected values of $\mathrm{CM}_{A_1}^+, \mathrm{CM}_{A_2}^-, \mathrm{CM}_A^+$ as computed in Example 3.23, and equal to $h_{A_1}, 1 - h_{A_1}, h_A$, respectively. $\triangleleft$

4.3 Hierarchical Multi-Label Classification

When dealing with HMC problems, the above implementation can be simplified. Indeed, in the hierarchical case, we have that all constraints have only one class in the body, all constraints are definite and thus $s = 1$.

Let H be an $l \times l$ matrix obtained by stacking l times CM_0. Let M be an $l \times l$ matrix such that, for $i, j \in \{1, \ldots, n\}$, $M_{ij} = 1$ if A_j is a subclass of A_i, and $M_{ij} = 0$, otherwise. The constraint module can be simply computed as:

$$\mathrm{CM}_s = \max(H \odot M, \dim = 1)\,,$$

For CLoss, we can use the same mask M to modify the standard BCELoss. In detail, let y be the ground-truth vector, and H' be the $l \times l$ matrix obtained by stacking l times the vector $\mathrm{CM}_s \odot y$. Then,

$$\mathrm{CLoss} = \mathrm{BCELoss}\big(((1 - y) \odot \mathrm{CM}_s) + (y \odot \max(M \odot H', \dim = 1)), y\big).$$

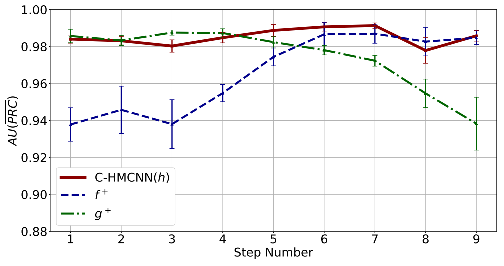

Figure 7: Mean $AU(\overline{PRC})$ with standard deviation of CCN(h), f^+, and g^+ for each step.

5. Experimental Analysis

In this section, we present the results of the experimental analysis. We first present our results focusing on HMC problems, and then we present the results obtained in the more general framework of LCMC problems. In the presentation, we always speak about CCN(h) since, given Theorem 3.25, in the case of HMC problems there is no difference between CCN(h) and C-HMCNN(h).

5.1 Hierarchical Multi-Label Classification

In this section, we present the experimental results of CCN(h), first considering two synthetic experiments, and then on 20 real-world datasets for which we compare with current state-of-the-art models for HMC problems. Finally, ablation studies highlight the positive impact of both CM and CLoss on CCN(h)'s performance.[4]

For evaluating performance, we consider the area under the average precision and recall curve $AU(\overline{PRC})$,[5] which is the most used metric in the HMC literature (Bi & Kwok, 2011; Vens et al., 2008; Wehrmann et al., 2018).

5.1.1 Synthetic Experiment 1

Consider the generalization of the experiment in Section 2.2 in which we started with R_1 outside R_2 (as in the second row of Figure 1), and then moved R_1 towards the centre of R_2 (as in the first row of Figure 1) in 9 uniform steps. The last row of Figure 1 corresponds to the fifth step, that is, R_1 was halfway. This experiment is meant to show how the performance of CCN(h), f^+, and g^+ defined as in Section 2.2 vary depending on the relative positions of R_1 and R_2. Here, f, g, and h were implemented and trained as in Section 2.2. For each step, we run the experiment 10 times,[6] and we plot the mean $AU(\overline{PRC})$ together with the standard deviation for CCN(h), f^+, and g^+ in Figure 7.

As expected, Figure 7 shows that f^+ performed poorly in the first three steps when $R_1 \cap R_2 = \emptyset$, it then started to perform better at step 4 when $R_1 \cap R_2 \notin \{R_1, \emptyset\}$, and it performed well from step 6 when R_1 overlaps significantly with R_2 (at least 65% of its area). Conversely, g^+ performed well on the first five steps, and its performance started

4. Link: https://github.com/EGiunchiglia/C-HMCNN/
5. $AU(\overline{PRC})$ is computed using the average precision method as implemented by Pedregosa et al. (2011).
6. All subfigures in Figure 1 correspond to the decision boundaries of f, g, and h in the first of the 10 runs.

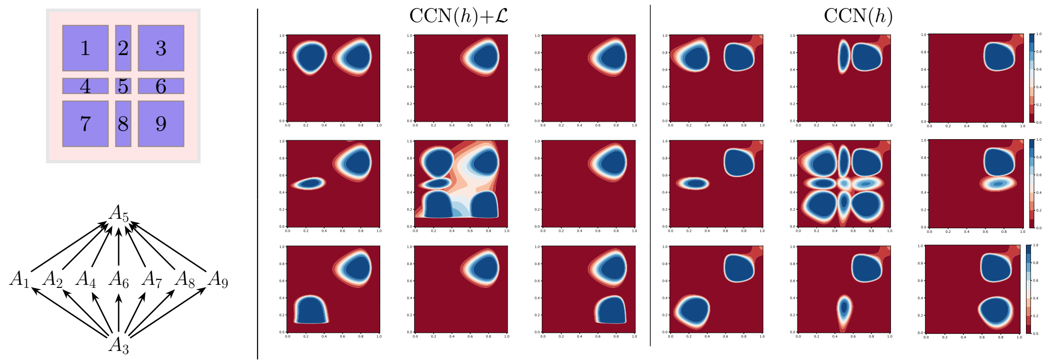

Figure 8: First column: rectangles disposition above and hierarchy representation below. Second column: decision boundaries of CCN(h)+$\mathcal{L}$ for each class. Last column: decision boundaries of CCN(h) for each class. In each figure showing decision boundaries, the darker the blue (resp., red), the more confident a model is that the data points in the region belong (resp., do not belong) to the class (see the scale at the end of each row).

decaying from step 6. CCN(h) performed well at all steps, as expected, showing robustness with respect to the relative positions of R_1 and R_2. Further, CCN(h) exhibits much more stable performances than f^+ and g^+ as highlighted by the visibly much smaller standard deviations of CCN(h).

5.1.2 Synthetic Experiment 2

In order to prove the importance of using CLoss instead of the standard binary cross entropy loss $\mathcal{L}$, in this experiment, we compare two models: (i) our model CCN(h), and (ii) $h+$CM, that is h with CM built on top and trained with $\mathcal{L}$. Consider the nine rectangles arranged as showed on the top left of Figure 8 named $R_1, \ldots, R_9$. Assume that

1. we have classes $A_1 \ldots A_9$,

2. a data point belongs to A_i if it belongs to the ith rectangle, and

3. A_5 (resp., A_3) is an ancestor (resp., descendant) of every class, as shown in the hierarchy on the bottom left of Figure 8.

Thus, all points in R_3 belong to all classes, and if a data point belongs to a rectangle, then it also belongs to class A_5. The datasets consisted of 5000 (50/50 train/test split) data points sampled from a uniform distribution over $[0,1]^2$.

Let h be a feedforward neural network with a single hidden layer with 7 neurons. We train both $h+$CM and CCN(h) for 20k epochs using Adam optimization with learning rate 10^{-2} ($\beta_1 = 0.9, \beta_2 = 0.999$). As expected, the average $AU(\overline{PRC})$ (and standard deviation) over 10 runs for $h+$CM trained with $\mathcal{L}$ is 0.938 (0.038), while $h+$CM trained with CLoss (CCN(h)) is 0.974 (0.007). Notice that not only $h+$CM performs worse, but also, due to the convergence to bad local optima, the standard deviation obtained with $h+$CM is 5 times higher than the one of CCN(h): the (min, median, max) $AU(\overline{PRC})$ for $h+$CM are $(0.871, 0.945, 0.990)$, while for CCN(h) are $(0.964, 0.975, 0.990)$. The difference between CCN(h) and CCN(h)+$\mathcal{L}$ in performance is further highlighted in Figure 8, which shows

Taxonomy	Dataset	D	n	Train	Val	Test
FunCat (FUN)	Cellcycle	77	499	1625	848	1281
FunCat (FUN)	Derisi	63	499	1605	842	1272
FunCat (FUN)	Eisen	79	461	1055	529	835
FunCat (FUN)	Expr	551	499	1636	849	1288
FunCat (FUN)	Gasch1	173	499	1631	846	1281
FunCat (FUN)	Gasch2	52	499	1636	849	1288
FunCat (FUN)	Seq	478	499	1692	876	1332
FunCat(FUN)	Spo	80	499	1597	837	1263
Gene Ontology (GO)	Cellcycle	77	4122	1625	848	1281
Gene Ontology (GO)	Derisi	63	4116	1605	842	1272
Gene Ontology (GO)	Eisen	79	3570	1055	528	835
Gene Ontology (GO)	Expr	551	4128	1636	849	1288
Gene Ontology (GO)	Gasch1	173	4122	1631	846	1281
Gene Ontology (GO)	Gasch2	52	4128	1636	849	1288
Gene Ontology (GO)	Seq	478	4130	1692	876	1332
Gene Ontology (GO)	Spo	80	4166	1597	837	1263
Tree	Diatoms	371	398	1085	464	1054
Tree	Enron	1000	56	692	296	660
Tree	Imclef07a	80	96	7000	3000	1006
Tree	Imclef07d	80	46	7000	3000	1006

Table 1: Summary of the 20 real-world datasets. Number of features (D), number of classes (n), and number of data points for each dataset split.

the decision boundaries of the 6th best performing networks.[7] The figure points out how mistakes given by wrong supervisions in lower levels of the hierarchy (see decision boundaries for A_2, A_6, and A_8) might have dramatic consequences in upper levels of the hierarchy (see decision boundaries for A_5).

5.1.3 Comparison with the State-of-the-Art

We tested CCN(h) on 20 real-world datasets commonly used to compare HMC systems (see, e.g., Bi & Kwok, 2011; Nakano et al., 2019; Vens et al., 2008; Wehrmann et al., 2018): 16 are functional genomics datasets (Clare, 2003), 2 contain medical images (Dimitrovski et al., 2008), 1 contains images of microalgae (Dimitrovski et al., 2012), and 1 is a text categorization dataset (Klimt & Yang, 2004).[8] The characteristics of these datasets are summarized in Table 1. These datasets are particularly challenging, because their number of training samples is rather limited, and they have a large variation, both in the number of features (from 52 to 1000) and in the number of classes (from 56 to 4130). We applied the same preprocessing to all the datasets. All the categorical features were transformed using one-hot encoding. The missing values were replaced by their mean in the case of numeric features and by a vector of all zeros in the case of categorical ones. All the features were standardized.

7. We picked the 6th best performing networks due to the high variance of the results CCN(h)+$\mathcal{L}$.
8. Links: https://dtai.cs.kuleuven.be/clus/hmcdatasets and http://kt.ijs.si/DragiKocev/PhD/resources

Dataset	CCN(h)	HMC-LMLP	Clus-Ens	Baseline	HMCN-R	HMCN-F
Cellcycle FUN	**0.255**	0.207	0.227	0.018	0.247	0.252
Derisi FUN	**0.195**	0.182	0.187	0.018	0.189	0.193
Eisen FUN	**0.306**	0.245	0.286	0.020	0.298	0.298
Expr FUN	**0.302**	0.242	0.271	0.018	0.300	0.301
Gasch1 FUN	**0.286**	0.235	0.267	0.018	0.283	0.284
Gasch2 FUN	**0.258**	0.211	0.231	0.018	0.249	0.254
Seq FUN	**0.292**	0.236	0.284	0.017	0.290	0.291
Spo FUN	**0.215**	0.186	0.211	0.018	0.210	0.211
Cellcycle GO	**0.413**	0.361	0.387	0.008	0.395	0.400
Derisi GO	**0.370**	0.343	0.361	0.008	0.368	0.369
Eisen GO	**0.455**	0.406	0.433	0.010	0.435	0.440
Expr GO	0.447	0.373	0.422	0.008	0.450	**0.452**
Gasch1 GO	**0.436**	0.380	0.415	0.008	0.416	0.428
Gasch2 GO	0.414	0.371	0.395	0.008	0.463	**0.465**
Seq GO	0.446	0.370	0.438	0.008	0.443	**0.447**
Spo GO	**0.382**	0.342	0.371	0.008	0.375	0.376
Diatoms	**0.758**	-	0.501	0.005	0.514	0.530
Enron	**0.756**	-	0.696	0.010	0.710	0.724
Imclef07a	**0.956**	-	0.803	0.031	0.904	0.950
Imclef07d	**0.927**	-	0.881	0.065	0.897	0.920
Avg Rank	1.25	5.00	3.93	6.00	2.93	1.90

Table 2: Comparison of CCN(h) with the other state-of-the-art models. The performance of each system is measured as the $AU(\overline{PRC})$ obtained on the test set. The best results are in bold.

We built h as a feedforward neural network with two hidden layers and ReLU non-linearity. To prove the robustness of CCN(h), we kept all the hyperparameters fixed except the hidden dimension and the learning rate used for each dataset, which are given in Appendix A and were optimized over the validation sets. In all experiments, the loss was minimized using Adam optimizer with weight decay 10^{-5}, and patience 20 ($\beta_1 = 0.9$, $\beta_2 = 0.999$). The dropout rate was set to 70% and the batch size to 4. As in the work by Wehrmann et al. (2018), we retrained CCN(h) on both training and validation data for the same number of epochs, as the early stopping procedure determined was optimal in the first pass.

For each dataset, we run CCN(h), Clus-Ens (Schietgat et al., 2010), and HMC-LMLP (Cerri et al., 2016) 10 times, and the average $AU(\overline{PRC})$ is reported in first three columns of Table 2. For simplicity, we omit the standard deviations, which for CCN(h) are in the range $[0.5 \times 10^{-3}, 2.6 \times 10^{-3}]$, proving that it is a very stable model. As reported by Nakano et al. (2019), Clus-Ens and HMC-LMLP are the current state-of-the-art models with publicly available code. These models were run on CPU (as there is no GPU implementation publicly available) with the suggested configuration settings on each dataset.[9] In the fourth column,

9. We also ran the code by Masera and Blanzieri (2018). However, we obtained very different results from the ones reported in the paper. Similar negative results are also reported by Nakano et al. (2019).

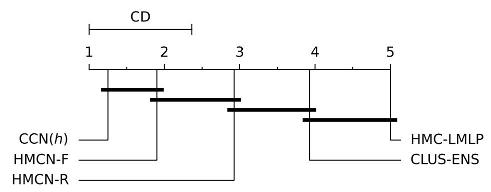

Figure 9: Critical diagram for the Nemenyi's statistical test.

we report the performance of a random performance classifier. As described by Saito and Rehmsmeier (2015), we computed the $AU(\overline{PRC})$ of such a random baseline by dividing the number of positive examples in the test set by the multiplication of the number of datapoints in the test set and the number of classes. In the last two columns, we show the results of HMCN-R and HMCN-F directly taken from (Wehrmann et al., 2018), since the code is not publicly available. We report the results of both systems, because, while HMCN-R has worse results than HMCN-F, the amount of parameters of the latter grows with the number of hierarchical levels. As a consequence, HMCN-R is much lighter in terms of total amount of parameters, and the authors advise that for very large hierarchies, HMCN-R is probably a better choice than HMCN-F considering the trade-off performance vs. computational cost (Wehrmann et al., 2018). Note that the number of parameters of CCN(h) is independent from the number of hierarchical levels.

As reported in Table 2, CCN(h) has the greatest number of wins (it has the best performance on all datasets but 3) and best average ranking (1.25). We also verified the statistical significance of the results following the instructions given in the work by Demsar (2006).[10] We first executed the Friedman test, obtaining p-value 4.26×10^{-15}. We then performed the post-hoc Nemenyi test, and the resulting critical diagram is shown in Figure 9, where the group of methods that do not differ significantly (significance level 0.05) are connected through a horizontal line. The Nemenyi test is powerful enough to conclude that there is a statistical significant difference between the performance of CCN(h) and all the other models but HMCN-F. Hence, as advised by Demsar (2006) and Benavoli et al. (2016), we compared CCN(h) and HMCN-F using the Wilcoxon test. This test, contrarily to the Friedman test and the Nemenyi test, takes into account not only the ranking, but also the differences in performance of the two algorithms. The Wilcoxon test allows us to conclude that there is a statistical significant difference between the performance of CCN(h) and HMCN-F with p-value of 6.01×10^{-3}.

To better understand why CCN(h) is able to outperform the other models, Figure 10 shows the average $AU(\overline{PRC})$ per hierarchy level achieved by CCN(h), Clus-HMC, and HMC-LMLP in each of the Funcat datasets.[11] The figure shows that CCN(h) is able to get better results than Clus-HMC and HMC-LMLP at all levels of the hierarchy for all the datasets (with the exception of levels 4 and 5 for the dataset Seq Fun, where Clus-HMC manages to outperform CCN(h)). Interestingly, we get the biggest gaps in performance at higher levels of the hierarchy. This is not surprising given that CLoss penalizes errors more

10. We exclude the baseline model, as its results significantly worse than all the others.
11. In Figure 10, the levels start at 1 because the root is not taken into account for evaluation. We could not measure the performance of HMCN-R and HMCN-F as the code is not available.

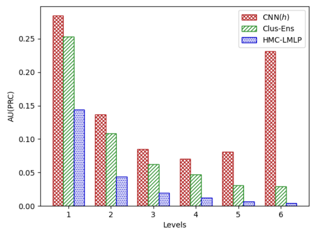

(a) Cellcycle FUN

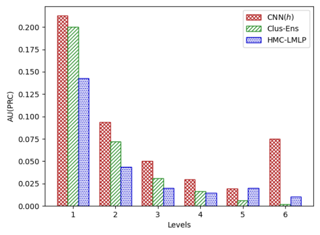

(b) Derisi FUN

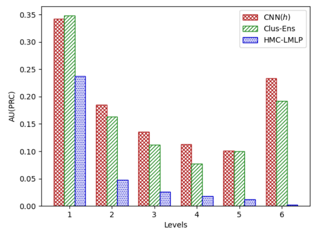

(c) Eisen FUN

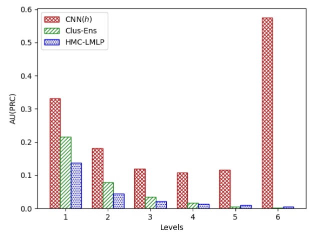

(d) Expr FUN

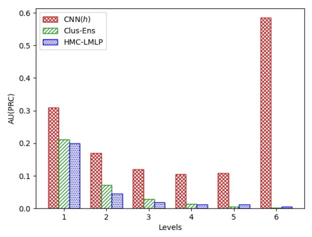

(e) Gasch1 FUN

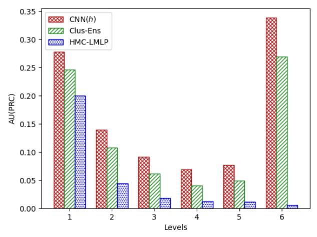

(f) Gasch2 FUN

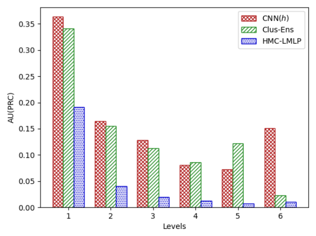

(g) Seq FUN

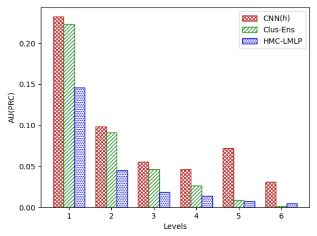

(h) Spo FUN

Figure 10: Average $AU(\overline{PRC})$ per hierarchy level.

at the higher levels. As an example, if at training time CCN(h) delegates the prediction of class A belonging to level 1 to class B belonging to level 6, then the error made by h_B will be counted 6 times in the loss, while the error made by h_A will not be counted at all.

Furthermore, to study how the models perform once a threshold is fixed, we compared CCN(h), Clus-HMC, and HMC-LMLP in terms of F1-score. For each model and dataset, we picked the threshold that maximizes the F1-score. The results are reported in Table 3, and show that CCN(h) is able to outperform HMC-LMLP and Clus-HMC on all datasets. In order to test the statistical significance of the results, we performed the Wilcoxon test, obtaining the p-value 3.1×10^{-5} when comparing CCN(h) and HMC-LMLP, and p-value 1.9×10^{-6} when comparing CCN(h) and Clus-HMC.

5.1.4 Ablation Studies

To analyze the impact of both CM and CLoss, we compared the performance of CCN(h) on the FunCat datasets against the performance of h^+, that is h with CM applied as post-processing at inference time and h+CM, that is h with CM built on top. Both these models were trained using the standard binary cross-entropy loss. As it can be seen in Table 4,

Dataset	CCN(h)	HMC-LMLP	Clus-Ens
Cellcycle FUN	**0.373**	0.251	0.292
Derisi FUN	**0.337**	0.251	0.265
Eisen FUN	**0.402**	0.262	0.336
Expr FUN	**0.401**	0.249	0.278
Gasch1 FUN	**0.392**	0.253	0.278
Gasch2 FUN	**0.377**	0.250	0.293
Seq FUN	**0.404**	0.242	0.330
Spo FUN	**0.346**	0.248	0.276
Cellcycle GO	**0.507**	0.396	0.420
Derisi GO	**0.481**	0.391	0.405
Eisen GO	**0.529**	0.410	0.422
Expr GO	**0.485**	0.393	0.416
Gasch1 GO	**0.523**	0.396	0.418
Gasch2 GO	**0.510**	0.395	0.417
Seq GO	**0.499**	0.374	0.425
Spo GO	**0.489**	0.391	0.418
Diatoms	**0.819**	-	0.502
Enron	**0.733**	-	0.636
Imclef07a	**0.924**	-	0.727
Imclef07d	**0.887**	-	0.804
Average Ranking	1.0	3.0	2.0

Table 3: Comparison of CCN(h) with the other state-of-the-art models. The performance of each system is measured as the F1-score obtained on the test set. The best results are in bold.

CCN(h), by exploiting both CM and CLoss, always outperforms h^+ and $h+$CM on all datasets. In Table 4, we also report after how many epochs the algorithm stopped training in average. As it can be seen, CCN(h), $h+$CM and h^+ always require approximately the same number of epochs.

5.2 Multi-Label Classification with Logical Hard Constraints

As for the hierarchical case, we first consider a generalization of the synthetic experiment proposed in the basic case. Then we test CCN(h) on 16 real-world datasets with general constraints, and finally we present the ablation studies.[12]

About the metrics, the analysis of 64 papers on MC problems conducted by Spolaôr et al. (2013) and reported by Pereira et al. (2018), shows that already in 2013 as many as 19 different metrics have been used to evaluate MC models, and still today different papers use different subsets of such metrics. However, as suggested by Pereira et al. (2018), not all subsets can be used, as the experimental results may appear to favor a specific behavior depending on the subset of measures chosen, thus possibly leading to misleading conclusions. To avoid such undesired results, the authors conducted a correlation analysis

12. Link: https://github.com/EGiunchiglia/CCN/

	h^+		h+CM		CCN(h)	
Dataset	$AU(\overline{PRC})$	Epochs	$AU(\overline{PRC})$	Epochs	$AU(\overline{PRC})$	Epochs
Cellcycle	0.240	107	0.238	108	**0.255**	106
Derisi	0.190	64	0.188	66	**0.195**	67
Eisen	0.290	112	0.286	107	**0.306**	110
Expr	0.272	39	0.267	19	**0.302**	20
Gasch1	0.265	41	0.262	42	**0.286**	38
Gasch2	0.244	128	0.242	132	**0.258**	131
Seq	0.249	13	0.252	13	**0.292**	13
Spo	0.201	108	0.202	117	**0.215**	115
Average Ranking	2.94		2.06		1.00	

Table 4: Impact of CM and CM+CLoss on the performance measured as $AU(\overline{PRC})$ and on the total number of epochs for the validation set of the Funcat datasets.

of the metrics that led to the individuation of clusters of correlated measures and thus to the proposal of various subsets of metrics, chosen according to the following criteria:

1. first, Hamming loss is highly recommended for inclusion in each subset: it is not correlated with others, and is the most used metric in the literature (55 papers out of the 64 surveyed),
2. next it could be considered employing other measures not correlated with any others like coverage error and ranking loss, and
3. finally, a suitable selection should include at least one metric from each cluster of correlated measures. Among them, multi-label accuracy is a good choice because it is among the ones with the highest correlations to other measures.

Other criteria they suggest and use for the selection of the proposed subsets are: popularity in the literature, the choice to include or not AUC-based metrics, and the size of the resulting set of metrics.

Following the above criteria, we used the following six metrics, each taking value in the interval $[0, 1]$ and each annotated with either $\uparrow$ or $\downarrow$ to mean that larger values for that metric stand for better (resp. worse) performance:

1. average precision ($\uparrow$),
2. coverage error ($\downarrow$),
3. Hamming loss ($\downarrow$),
4. multi-label accuracy ($\uparrow$),
5. one-error ($\downarrow$), and
6. ranking loss ($\downarrow$).

The above six metrics are exactly those belonging to the first two subsets of metrics proposed by Pereira et al. (2018).[13] Notice that, the above list does not include $AU(\overline{PRC})$: already

13. In particular, the first of the proposed subsets includes coverage error, Hamming loss, multi-label accuracy and ranking loss, while the second includes average precision, coverage error, Hamming loss, one-error and ranking loss; see (Pereira et al., 2018) for more details.

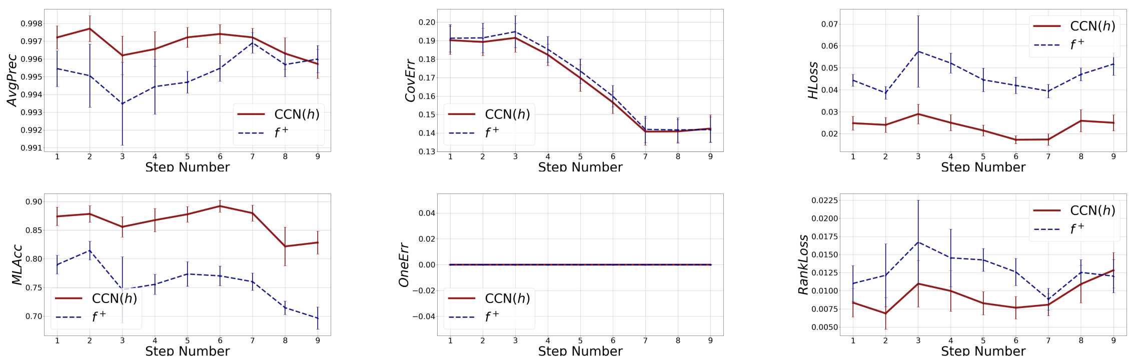

Figure 11: Mean average precision, coverage error, hamming loss, multi-label accuracy, one-error, and ranking loss with standard deviation of CCN(h) and f^+ for each step.

in 2013 and still today, contrarily to the specialized HMC literature, it is generally not used in the MC literature (Spolaôr et al., 2013; Pereira et al., 2018; Feng et al., 2019).

5.2.1 Synthetic Experiment

Consider the generalization of the experiment presented as basic case, in which we started with R_1 outside R_2 (as in the first row of Fig. 3), and then moved R_1 towards the centre of R_2 (as in the second row of Fig. 3) in 9 uniform steps. As for HMC problems, this experiment is meant to show how the performance of CCN(h) and f^+ defined as in Section 3.2 vary depending on the relative positions of R_1 and R_2. As expected, Figure 11 shows that CCN(h) performs better or equally to f^+ at all steps and for all metrics. In particular:

- CCN(h) performs consistently better than f^+ at all steps in terms of average precision, coverage error, Hamming loss, multi-label accuracy and ranking loss. Further, as in the HMC case, CCN(h) exhibits much more stable performances than f^+ as highlighted by the visibly much smaller standard deviation bar of CCN(h).

- CCN(h) and f^+ perform identically in terms of one-error. This is due to the fact that one-error measures the fraction of instances whose most confident class is irrelevant, since neither CCN(h) nor f^+ ever make this mistake, they both have one-error equal to zero at all steps.

5.3 Comparison with the State-of-the-Art

In order to prove the superiority of our model, we adopted the same methodology presented in (Feng et al., 2019) and consider the three well-established MC models and the state-of-the-art MC model tested in (Feng et al., 2019), which can be characterized by the order of classes correlations they exploit. Thus, CCN(h) is compared with

1. BR (Boutell et al., 2004), a first order model which considers each class separately, ignoring class correlations, and

Dataset	D	L	Train	Val	Test	C	H	B	B^+	B^-	H/L
Arts	462	26	2975	525	1500	344	11	7.1	5.6	1.5	42.3%
Bibtex	1836	159	4148	732	2515	399	32	4.2	4.2	0.0	20.1%
Business	438	30	2975	525	1500	77	7	2.5	2.3	0.2	23.3%
Cal500	68	174	298	53	151	39	7	2.0	1.1	0.9	4.0%
Delicious	500	983	10982	1938	3185	104	61	1.0	1.0	0.0	6.1%
Emotions	72	6	332	59	202	1	1	5.0	0.0	5.0	16.7%
Enron	1001	53	954	169	579	7	5	1.0	1.0	0.0	9.4%
Genbase	1186	27	393	70	199	88	13	2.2	2.0	0.2	48.1%
Image	294	5	1190	210	600	1	1	4.0	0.0	4.0	20.0%
Medical	1449	45	283	50	645	17	9	1.2	1.2	0.0	20.0%
Rcv1subset1	944	101	3570	630	1800	247	16	3.7	2.9	0.8	15.8%
Rcv1subset2	944	101	3570	630	1800	81	15	2.4	1.7	0.7	14.9%
Rcv1subset3	944	101	3570	630	1800	72	16	2.3	1.7	0.6	15.8%
Rcv1subset4	944	101	3570	630	1800	63	14	2.1	1.7	0.4	13.9%
Rcv1subset5	944	101	3570	630	1800	73	11	2.5	2	0.5	10.9%
Science	743	40	2975	525	1500	37	11	2.1	1.7	0.4	27.5%
Scene	294	6	1029	182	1196	1	1	5.0	0.0	5.0	16.7%
Yeast	103	14	1275	225	917	34	11	2.3	1.9	0.4	78.6%

Table 5: Summary of the real-world MC datasets. For each dataset, we report from left to right: (i) name, (ii) number of features (D), (iii) number of classes (L), (iv-vi) number of data points for each split, (vii) number of constraints (C), (iix) number of different classes that appear at least once as head of a constraint (H), (ix) average number of classes appearing in the body (B), (x-xi) average number of classes appearing positively (resp., negatively) in the body (B^+), (resp., (B^-)), and (xii) percentage of classes appearing at least once as head of a constraint.

2. ECC (Read et al., 2009), RAKEL (Tsoumakas et al., 2009) and CAMEL (Feng et al., 2019), which exploit correlations among two or more classes.

BR, ECC, and RAKEL are the well-established MC models, and CAMEL is the current state-of-the-art MC model (Feng et al., 2019). Since these models are not guaranteed to output predictions that are coherent with the constraints, we applied CM as additional post-processing steps.

Being the first paper on LCMC problems, we created 16 real-world LCMC datasets, each obtained by enriching a popular and publicly available MC dataset with constraints extracted using the apriori algorithm (Agrawal & Srikant, 1994). The apriori algorithm is the standard algorithm used for association rules mining. We run it with the following hyperparameters: (i) confidence (i.e., the ratio of datapoints for which the constraint holds true) equal to 1, (ii) minimum support (i.e., the ratio of datapoints for which the body holds true) equal to 0, and (iii) max itemset (i.e., the maximum number of elements allowed in the body and in the head) equal to 5. We then pruned the set of returned constraints to obtain a set of stratified normal rules. The list of the datasets together with a summary of their characteristics is reported in Table 5. The various datasets come from different application domains, in particular:

Model	Arts	Bibtex	Business	Cal500	Delicious	Emotions	Enron	Genbase	Image
				Average precision (↑)					
CCN(h)	0.623	0.586	**0.904**	**0.520**	0.347	**0.800**	0.704	0.996	**0.807**
CAMEL	**0.625**	**0.605**	0.899	0.513	**0.398**	0.756	**0.708**	0.990	0.793
ECC	0.544	0.302	0.867	0.401	0.112	0.772	0.643	**1.000**	0.738
BR	0.546	0.308	0.863	0.441	0.140	0.793	0.643	**1.000**	0.726
RAKEL	0.530	0.317	0.856	0.433	0.140	0.798	0.636	**1.000**	0.721
				Coverage error (↓)					
CCN(h)	**0.172**	**0.105**	**0.065**	**0.734**	**0.520**	**0.315**	**0.217**	0.016	**0.187**
CAMEL	0.202	0.157	0.083	0.791	0.613	0.372	0.256	0.010	0.201
ECC	0.223	0.801	0.089	0.853	0.987	0.338	0.285	**0.009**	0.242
BR	0.217	0.802	0.086	0.789	0.989	0.324	0.288	**0.009**	0.245
RAKEL	0.221	0.796	0.085	0.791	0.988	0.317	0.294	**0.009**	0.250
				Hamming loss (↓)					
CCN(h)	**0.054**	**0.013**	**0.023**	**0.136**	**0.018**	**0.197**	**0.046**	**0.001**	**0.172**
CAMEL	0.055	**0.013**	**0.023**	0.138	**0.018**	0.265	0.047	0.003	0.174
ECC	0.081	**0.013**	0.031	0.172	0.019	0.245	0.055	**0.001**	0.218
BR	0.079	**0.013**	0.032	0.162	**0.018**	0.229	0.054	**0.001**	0.232
RAKEL	0.082	**0.013**	0.034	0.165	0.019	0.223	0.055	**0.001**	0.225
				Multi-label accuracy (↑)					
CCN(h)	**0.238**	**0.272**	0.601	0.203	0.905	**0.534**	**0.395**	0.986	**0.488**
CAMEL	0.218	0.193	**0.609**	0.210	0.147	0.354	0.381	0.943	0.456
ECC	0.217	0.250	0.548	0.220	0.114	0.446	0.361	**0.992**	0.387
BR	0.217	0.260	0.538	0.221	0.150	0.465	0.365	**0.992**	0.369
RAKEL	0.215	0.263	0.527	**0.222**	**0.152**	0.485	0.361	**0.992**	0.376
				One-error (↓)					
CCN(h)	0.475	0.376	0.093	**0.113**	0.357	**0.273**	0.235	**0.000**	**0.296**
CAMEL	**0.460**	**0.349**	**0.090**	0.133	**0.315**	0.381	**0.223**	0.020	0.310
ECC	0.568	0.535	0.137	0.378	0.692	0.332	0.309	**0.000**	0.392
BR	0.567	0.517	0.147	0.232	0.546	0.292	0.299	**0.000**	0.425
RAKEL	0.586	0.513	0.159	0.232	0.567	0.292	0.304	**0.000**	0.430
				Ranking loss (↓)					
CCN(h)	**0.115**	**0.058**	**0.030**	**0.173**	**0.110**	**0.161**	**0.076**	0.003	**0.159**
CAMEL	0.136	0.078	0.040	0.189	0.117	0.237	0.086	**0.001**	0.177
ECC	0.158	0.680	0.046	0.257	0.861	0.193	0.107	**0.001**	0.231
BR	0.155	0.670	0.045	0.218	0.820	0.177	0.108	**0.001**	0.234
RAKEL	0.159	0.659	0.044	0.220	0.815	0.169	0.112	**0.001**	0.242

Table 6: Comparison of CCN(h) with the other state-of-the-art models. The best results are in bold.

Model	Medical	Rcv1S1	Rcv1S2	Rcv1S3	Rcv1S4	Rcv1S5	Science	Scene	Yeast
					Average precision (↑)				
CCN(h)	**0.866**	**0.642**	**0.666**	**0.647**	**0.675**	0.560	0.603	**0.868**	**0.768**
CAMEL	0.807	0.622	0.647	0.636	0.654	**0.564**	**0.614**	0.824	0.766
ECC	0.823	0.549	0.575	0.585	0.609	0.529	0.502	0.794	0.724
BR	0.823	0.536	0.563	0.572	0.600	0.524	0.500	0.781	0.743
RAKEL	0.811	0.532	0.556	0.562	0.589	0.508	0.493	0.794	0.732
					Coverage error (↓)				
CCN(h)	**0.035**	**0.092**	**0.089**	**0.103**	**0.080**	**0.107**	**0.131**	**0.077**	**0.452**
CAMEL	0.036	0.131	0.115	0.123	0.103	0.130	0.162	0.106	0.457
ECC	0.045	0.185	0.166	0.167	0.169	0.196	0.225	0.127	0.495
BR	0.045	0.194	0.181	0.178	0.184	0.210	0.227	0.128	0.476
RAKEL	0.049	0.201	0.180	0.185	0.195	0.209	0.225	0.123	0.481
					Hamming loss (↓)				
CCN(h)	**0.013**	**0.026**	**0.022**	**0.024**	**0.019**	**0.025**	**0.031**	**0.092**	**0.196**
CAMEL	0.024	0.027	**0.022**	**0.024**	0.021	**0.025**	**0.031**	0.109	**0.196**
ECC	0.019	0.031	0.027	0.028	0.026	0.030	0.049	0.131	0.221
BR	0.019	0.032	0.028	0.029	0.027	0.031	0.051	0.151	0.214
RAKEL	0.019	0.033	0.029	0.030	0.027	0.031	0.051	0.130	0.225
					Multi-label accuracy (↑)				
CCN(h)	**0.589**	**0.296**	**0.310**	**0.303**	**0.324**	**0.275**	**0.255**	**0.607**	**0.480**
CAMEL	0.284	0.204	0.222	0.210	0.257	0.223	0.217	0.528	**0.480**
ECC	0.481	0.264	0.277	0.273	0.297	0.269	0.209	0.478	0.443
BR	0.477	0.263	0.279	0.275	0.289	0.263	0.200	0.438	0.456
RAKEL	0.481	0.263	0.272	0.268	0.290	0.258	0.201	0.481	0.445
					One-error (↓)				
CCN(h)	**0.181**	**0.413**	**0.389**	**0.405**	**0.379**	**0.402**	0.494	**0.224**	0.234
CAMEL	0.285	**0.413**	0.397	0.413	0.399	0.414	**0.472**	0.287	**0.231**
ECC	0.251	0.477	0.462	0.453	0.436	0.451	0.603	0.319	0.300
BR	0.251	0.492	0.474	0.466	0.435	0.466	0.605	0.358	0.259
RAKEL	0.266	0.488	0.481	0.471	0.439	0.474	0.606	0.329	0.270
					Ranking loss (↓)				
CCN(h)	**0.024**	**0.036**	**0.035**	**0.046**	**0.035**	**0.046**	**0.094**	**0.073**	**0.172**
CAMEL	0.026	0.051	0.048	0.050	0.046	0.054	0.117	0.101	0.173
ECC	0.033	0.086	0.078	0.078	0.086	0.093	0.176	0.103	0.208
BR	0.032	0.091	0.088	0.085	0.097	0.101	0.177	0.131	0.190
RAKEL	0.037	0.093	0.088	0.089	0.103	0.102	0.180	0.127	0.200

Table 7: Comparison of CCN(h) with the other state-of-the-art models. The best results are in bold.

Metric	Average ranking					Friedman test	Wilcoxon test
	CCN(h)	CAMEL	ECC	BR	RAKEL	p-value	CCN(h) vs. CAMEL
Average precision	**1.50**	2.17	3.53	3.58	4.22	✓✓	
Coverage Error	**1.22**	2.36	3.61	3.92	3.89	✓✓	✓✓
Hamming loss	**1.36**	2.56	3.39	3.61	3.92	✓✓	✓✓
Multi-label accuracy	**1.69**	3.58	3.19	3.27	3.25	✓✓	✓✓
One-error	**1.50**	2.08	3.67	3.56	4.19	✓✓	
Ranking loss	**1.22**	2.19	3.61	3.72	4.17	✓✓	✓✓

Table 8: Average ranking for each metric and model, results of the Friedman and Wilcoxon test (the latter deployed to compare the performance of CCN(h) and CAMEL). We use ✓ (resp., ✓✓) to indicate that the test returned p-value < 0.05 (resp., < 0.01).

1. Cal500 and Emotions are 2 music classification datasets (Turnbull et al., 2008; Tsoumakas et al., 2008),

2. Genbase and Yeast are 2 functional genomics datasets (Diplaris et al., 2005; Elisseeff & Weston, 2001),

3. Image and Scene are 2 image classification datasets (Zhang & Zhou, 2007; Boutell et al., 2004), and

4. the remaining 10 are text classification datasets (Pestian et al., 2007; Read et al., 2008; Srivastava & Zane-Ulman, 2005; Tsoumakas & Vlahavas, 2007).[14]

Furthermore, as it can be seen from Table 5, they differ significantly both in the number of data points/classes (columns D and L) and in the characteristics of the associated sets of constraints. Indeed, we have datasets having just a few (one)/many constraints (column C), involving a few/many classes in the head (column H/L) and in the body, either positively or negatively (columns B, B^+ and B^-).

As in the HMC experiments, we applied the same preprocessing to all the datasets. All the categorical features were transformed using one-hot encoding. The missing values were replaced by their mean in the case of numeric features and by a vector of all zeros in the case of categorical ones. All the features were standardized. As in the HMC experiments, we built h as a feedforward neural network with two hidden layers and ReLU non-linearity. To prove the robustness of CCN(h), we kept all the hyperparameters fixed except the hidden dimension used for each dataset, which is given in Appendix B. Such hidden dimensions were optimized over the validation sets. In all experiments, the loss was minimized using Adam optimizer with batch size equal to 4, learning rate equal to 10^{-4}, and patience 20 ($\beta_1 = 0.9, \beta_2 = 0.999$). Since some datasets have very few data points, we set the dropout rate equal to 80% and the weight decay equal to 10^{-4}. As for the HMC case, we retrained CCN(h) on both training and validation data for the same number of epochs, as the early stopping procedure determined was optimal in the first pass. For each dataset, we run the models 10 times, and the average for each of the metrics is reported in Tables 6 and 7. For ease of presentation, we omit the standard deviations, which for CCN(h) are in the range

14. Link to datasets with constraints: https://github.com/EGiunchiglia/CCN/tree/master/data/

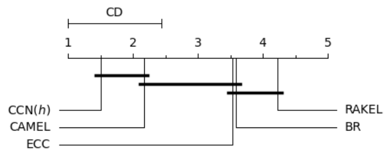

(a) Average precision

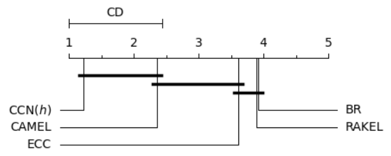

(b) Coverage error

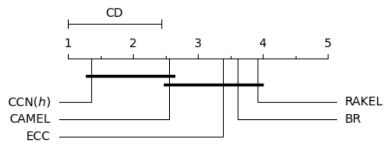

(c) Hamming loss

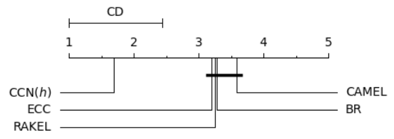

(d) Multi-label accuracy

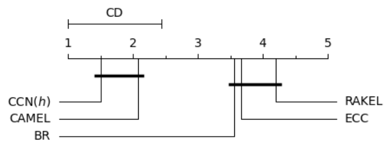

(e) One-error

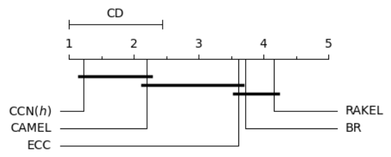

(f) Ranking loss

Figure 12: Critical diagram for each metric obtained with the post-hoc Nemenyi test.

$[2.9 \times 10^{-17}, 8.0 \times 10^{-3}]$, proving that it is a very stable model. ECC, BR, and RAKEL were implemented using scikit-multilearn (Szymanski & Kajdanowicz, 2017) by deploying the logistic regression model as the base classifier. Regarding CAMEL, we used the publicly available authors' implementation,[15] with the hyperparameters suggested by the authors. For all the models, we got results comparable to the ones reported in the work by Feng et al. (2019).

As it can be seen in Tables 6 and 7, CCN(h) has the highest number of wins in all metrics. Indeed, as it can be seen in Table 8, CCN(h) has the best average ranking in all metrics. We also verified the statistical significance of the results – as advised by Demsar (2006) – by performing the Friedman test for each metric. As reported in Table 8, the Friedman test returned p-value < 0.01 for each metric; we could thus proceed with the post-hoc Nemenyi tests, and the resulting critical diagrams are reported in Figure 12. In each diagram, the groups of methods that do not differ significantly (significance level 0.05) are connected through an horizontal line. According to the Nemenyi test, CCN(h)'s performance differs significantly to the performance of all the other models but CAMEL in terms of average precision, coverage error, Hamming loss, one-error and ranking loss, while it differs significantly to all the models (including CAMEL) in terms of multi-label accuracy. As in the HMC case, we then followed the guidelines given by Demsar (2006) and Benavoli et al. (2016) and performed the Wilcoxon test to compare the difference between CAMEL and CCN(h). As reported in the last column of Table 8, the performances of CCN(h) and CAMEL differ significantly for all metrics but one-error, thus further confirming the superiority of our model.

15. Link: https://github.com/hinanmu/CAMEL

Model	Arts	Bibtex	Business	Cal500	Delicious	Emotions	Enron	Genbase	Image
				Average precision (↑)					
CCN(h)	**0.623**	**0.586**	**0.904**	**0.520**	**0.347**	**0.800**	**0.704**	**0.996**	**0.807**
h^+	**0.623**	0.585	0.903	0.519	**0.347**	0.796	**0.704**	**0.996**	0.800
h+CM	**0.623**	0.580	0.902	0.519	0.344	**0.800**	**0.704**	0.978	**0.807**
				Coverage error (↓)					
CCN(h)	**0.172**	**0.105**	**0.065**	**0.734**	**0.520**	0.315	**0.217**	**0.016**	**0.187**
h^+	**0.172**	0.106	0.073	**0.734**	**0.520**	0.319	**0.217**	0.017	0.194
h+CM	0.173	0.108	0.072	**0.734**	**0.520**	**0.311**	**0.217**	0.020	**0.187**
				Hamming loss (↓)					
CCN(h)	**0.054**	**0.130**	**0.023**	**0.136**	**0.018**	**0.197**	**0.046**	**0.001**	0.172
h^+	**0.054**	**0.130**	0.026	**0.136**	**0.018**	0.201	**0.046**	**0.001**	0.172
h+CM	**0.054**	**0.130**	0.026	**0.136**	**0.018**	0.198	**0.046**	0.003	**0.169**
				Multi-label accuracy (↑)					
CCN(h)	**0.238**	**0.272**	**0.601**	**0.203**	0.095	**0.534**	**0.395**	**0.986**	**0.488**
h^+	**0.238**	**0.272**	**0.601**	**0.203**	**0.096**	0.512	**0.395**	**0.986**	0.475
h+CM	0.237	0.270	0.599	**0.203**	**0.096**	0.519	**0.395**	0.935	0.487
				One-error (↓)					
CCN(h)	**0.475**	**0.376**	**0.093**	**0.113**	**0.357**	**0.273**	**0.235**	**0.000**	**0.296**
h^+	0.476	0.384	**0.093**	**0.113**	**0.357**	0.283	0.238	**0.000**	0.307
h+CM	**0.475**	0.385	**0.093**	**0.113**	0.362	0.276	0.237	0.004	0.297
				Ranking loss (↓)					
CCN(h)	**0.115**	**0.058**	**0.030**	**0.173**	**0.110**	0.161	**0.076**	**0.003**	**0.159**
h^+	0.116	0.059	0.034	**0.173**	**0.110**	0.167	**0.076**	**0.003**	0.169
h+CM	0.116	0.060	0.034	**0.173**	**0.110**	**0.159**	**0.076**	0.006	0.160

Table 9: Results of the ablations studies. The best results are in bold.

5.4 Ablation Studies

As in the HMC case, in order to analyze the impact of both CM and CLoss, we compared the performance of CCN(h) against the performance of h^+, that is, h with the enforcement of the constraints done as a post-processing step, and $h + \text{CM}$, that is, h with CM built on top. Both these models were trained using the standard binary cross-entropy loss. The results of the ablation studies for each metric and each dataset are given in Tables 9 and 10, while the average ranking for each metric can be found in Table 11. As it can be seen in Table 11, CCN(h) has the highest average ranking for all metrics. Furthermore, we check the statistical significance of our results through the Wilcoxon test, whose results are reported in the last two columns of Table 11. As it can be seen, CCN(h) performs significantly better than h^+ for all metrics but multi-label accuracy. On the other hand, CCN(h) performs significantly better than $h + \text{CM}$ for all metrics but one-error.

Model	Medical	Rcv1S1	Rcv1S2	Rcv1S3	Rcv1S4	Rcv1S5	Science	Scene	Yeast
					Average precision (↑)				
CCN(h)	0.866	**0.642**	**0.666**	**0.647**	0.675	**0.560**	**0.603**	**0.868**	**0.768**
h^+	**0.868**	0.639	0.662	0.645	0.663	0.548	**0.603**	0.864	0.765
h+CM	0.864	0.630	0.663	0.640	**0.682**	**0.560**	0.602	0.867	0.767
					Coverage error (↓)				
CCN(h)	**0.035**	**0.092**	**0.089**	0.103	**0.080**	**0.107**	**0.131**	**0.077**	**0.452**
h^+	0.037	0.093	0.090	**0.102**	0.089	0.112	0.135	0.081	0.455
h+CM	0.037	**0.092**	0.090	0.103	0.089	0.115	0.135	0.078	0.453
					Hamming loss (↓)				
CCN(h)	**0.013**	**0.026**	**0.022**	**0.024**	**0.019**	**0.025**	**0.031**	**0.092**	**0.196**
h^+	0.015	0.027	0.023	0.025	0.022	0.027	0.032	**0.092**	**0.196**
h+CM	0.015	0.027	0.023	0.025	0.020	**0.025**	0.032	**0.092**	**0.196**
					Multi-label accuracy (↑)				
CCN(h)	0.589	**0.296**	**0.310**	0.303	**0.324**	0.275	0.255	**0.607**	0.480
h^+	**0.591**	**0.296**	0.309	**0.305**	0.323	**0.277**	**0.257**	0.603	**0.487**
h+CM	0.587	0.283	0.306	0.301	0.321	0.257	0.250	0.604	0.482
					One-error (↓)				
CCN(h)	**0.181**	**0.413**	**0.389**	**0.405**	0.379	**0.402**	**0.494**	**0.224**	0.234
h^+	**0.181**	**0.413**	0.396	**0.405**	0.394	0.420	**0.494**	0.227	0.234
h+CM	0.185	0.434	0.391	0.407	**0.357**	0.407	0.496	0.226	**0.231**
					Ranking loss (↓)				
CCN(h)	**0.024**	**0.036**	**0.035**	**0.046**	**0.035**	**0.046**	**0.094**	**0.073**	**0.172**
h^+	0.026	**0.036**	0.036	**0.046**	0.039	0.049	0.097	0.077	**0.172**
h+CM	0.025	0.037	0.037	0.047	0.039	0.049	0.096	0.074	0.174

Table 10: Results of the ablation studies. The best results are in bold.

6. Related Work

In this article, we introduced LCMC problems: MC problems in which every prediction must satisfy a given set of hard constraints expressed as normal rules. HMC problems are special cases of LCMC in which the body of each constraint is a single class and with the additional restriction that the graph associated to the set of constraints is acyclic.

We divide this section on the related work into two parts: in the first part, we focus on the literature in the HMC field, while in the second part, we present and discuss the previous works that have already dealt with the problem of imposing more expressive constraints on MC problems.

6.1 Hierarchical Multi-Label Classification

In the literature, HMC methods are traditionally divided into local and global approaches (Silla & Freitas, 2011).

Metric	Average ranking			Wilcoxon test	
	CCN(h)	h^+	h+CM	CCN(h) vs. h^+	CCN(h) vs. h+CM
Average precision	**1.39**	2.28	2.33	✓✓	✓
Coverage error	**1.39**	2.36	2.25	✓✓	✓
Hamming loss	**1.53**	2.33	2.14	✓✓	✓
Multi-label accuracy	**1.69**	1.72	2.58		✓✓
One-error	**1.44**	2.31	2.25	✓✓	✓
Ranking loss	**1.33**	2.28	2.39	✓✓	✓✓

Table 11: Average ranking for each metric and model, and results of the Wilcoxon test: ✓ (resp., ✓✓) is used to indicate that the Wilcoxon test returned p-value < 0.05 (resp., < 0.01).

Local approaches decompose the problem into smaller classification ones, and then the solutions are combined to solve the main task. Local approaches can be further divided based on the strategy that they deploy to decompose the main task. If a method trains a different classifier for each level of the hierarchy, then we have a *local classifier per level*, like the models proposed by Cerri et al. (2011, 2014, 2016), Li et al. (2018) and Zou et al. (2019). The works by Cerri et al. (2011, 2014, 2016) are extended by Wehrmann et al. (2018), who present HMCN-R and HMCN-F. Since HMCN-R and HMCN-F are trained with both a local loss and a global loss, they are considered hybrid local-global approaches. If a method trains a classifier for each node of the hierarchy, then we have a *local classifier per node*. Cesa-Bianchi et al. (2006) propose a linear classifier which is trained for each node with a loss function that captures the hierarchy structure. On the other hand, Feng et al. (2018) deploy one multi-layer perceptron for each node. A different approach is proposed in the work by Bi and Kwok (2011), where kernel dependency estimation is employed to project each class to a low-dimensional vector. To preserve the hierarchy structure, a generalized condensing sort and select algorithm is developed, and each vector is then learned singularly using ridge regression. Finally, if a method trains a different classifier per parent node in the hierarchy, then we have a *local classifier per parent node*. For example, Kulmanov et al. (2018) propose to train a model for each sub-ontology of the Gene Ontology, combining features automatically learned from the sequences and features based on protein interactions. Xu and Geng (2019), instead, try to solve the overfitting problem typical of local models by representing the correlation among the classes by the class distribution, and then training each local model to map data points to class distributions.

Global methods consist of single models able to map objects with their corresponding classes in the hierarchy as a whole. A well-known global method is Clus-HMC (Vens et al., 2008), consisting of a single predictive clustering tree for the entire hierarchy. This work is extended by Schietgat et al. (2010), who propose Clus-Ens: an ensemble of Clus-HMC. In Masera and Blanzieri (2018) propose a neural network incorporating the structure of the hierarchy in its architecture. While this network makes predictions that are coherent with the hierarchy, it also makes the assumption that each parent class is the union of the children. Borges and Nievola (2012) propose *competitive neural networks*, whose architecture replicates the hierarchy. The name of these networks comes from the fact that the neurons in the output layer compete with each other to be activated.

If we move the focus on how the satisfaction of the constraints is guaranteed, HMC models can be divided in:

1. approaches that satisfy the constraints by construction, and
2. approaches that require a post-processing step to enforce the constraints.

In the first category, we can find methods such as Clus-HMC (Vens et al., 2008), which is a decision tree and hence satisfies by construction each hierarchy constraint. Clus-Ens, the ensemble of Clus-HMC, computes the average of all class vectors predicted by the trees in the ensemble, and hence its predictions always satisfy the constraints. The model proposed by Bi and Kwok (2011), in order to preserve the hierarchy structure, develops a generalized condensing sort and select algorithm, while Cesa-Bianchi et al. (2006) evaluate the node classifiers in a top-down fashion, thus not making a prediction at all for the descendants of a node that has not been predicted.

Many of the neural-network-based models belong to the second category. A common policy to enforce the satisfaction of $A_1 \rightarrow A$ is to force the output for class A_1 to be smaller than or equal to the output for A (see, e.g., Cerri et al., 2011, 2014, 2016; Wehrmann et al., 2018). However, other solutions are possible. For example, Borges and Nievola (2012) associate to each data point an initial set of classes which is then extended to include all their ancestors in the hierarchy, while Feng et al. (2018) apply a post processing method based on Bayesian networks in order to guarantee that the results are coherent with the hierarchy constraints. For a detailed overview on the many different policies that can be used to impose the hierarchy constraints as a post-processing step, see the survey by Obozinski et al. (2008).

6.2 More Expressive Constraints

When dealing with more expressive constraints, researchers have mostly focused on the problem of exploiting them to improve their models and/or to deal with data scarcity, curiously neglecting the problem of guaranteeing their satisfaction.

If we focus on constraints expressed as logic rules, then we can find works such as the one by Hu et al. (2016a), in which the authors introduce an iterative method to embed structured information expressed by first order logic (FOL) formulas into the weights of different kinds of deep neural networks. At each step, they consider a *teacher network* based on the set of FOL rules to train a *student network* to fit both supervisions and logic rules. The work has been later extended to jointly learn the structure of the rules and their weights (Hu et al., 2016b). A different approach is considered by Li and Srikumar (2019), where a new framework is introduced to augment a neural network assigning semantics via logical rules to its neurons. Indeed, some neurons are associated with logical predicates, and then their activation is modified depending on the activation of the neurons corresponding to predicates that co-occur in the same rules. Many works embed logical constraints into penalty functions to formulate a learning problem (see e.g., Diligenti et al., 2017; Donadello et al., 2017; Xu et al., 2018). These works generally consider a fuzzy relaxation of FOL formulas to get a differentiable loss function that may be minimized by gradient descent. However, as the loss function is minimized, there is no guarantee that the constraints are fully satisfied.

If we further broaden our view to more general constraints, that is, to any constraint that enforces some correlation on the outputs of the model, then we can find a very wide literature, in which many works have shown that exploiting the background knowledge expressed by the constraints can bring some benefits. For example, Stewart and Ermon (2017) exploit the background knowledge coming from known laws of physics to train neural networks without any labeled example. Chen et al. (2015) combine Markov random fields with deep neural networks to express some context correlation in an image segmentation task. Similarly, Huang et al. (2015) consider conditional random fields on top of a bidirectional LSTM (Hochreiter & Schmidhuber, 1997) to enforce some statistical co-occurrencies (n-grams) among the network predictions, achieving state-of-the-art performance on POS and chunking tasks. Some of these works have also tried to impose hard constraints on learning algorithms, however, dealing effectively with hard constraints commonly requires a specific optimization schema, for example by considering a sequence of problems where the hard constraints are replaced by soft ones associated with larger and larger penalties, (see Bertsekas, 2014; Fletcher, 2013 for a detailed dissertation on optimization methods), and convergence is only guaranteed under suitable conditions; see the work by Luenberger (1997). Gnecco et al. (2014) consider different learning problems where both soft and hard constraints are taken into account at the same time. Soft constraints are added to the penalty function, while the optimal solution (if it exists) is required to satisfy a system of (in)equalities corresponding to the hard constraints. A newly devised approach to asymptotically satisfy hard constraints is considered by Farina et al. (2020), where the authors use the distributed asynchronous method of multipliers to solve the optimization problem. Another approach that can incorporate hard constraints are probabilistic sentential decision diagrams (Kisa et al., 2014). This approach (later extended by Shen et al., 2016, 2018, 2019) was designed to learn distributions over structured objects and to assign zero probability to outputs inconsistent with the constraints. It belongs to the framework of probabilistic circuits (Choi et al., 2020), whose models lend themselves to learning from a combination of data and background knowledge expressed in different ways (see, e.g., Poon & Domingos, 2011; Rahman et al., 2014.)

7. Conclusion

In this article, we introduced and dealt with LCMC problems: MC problems with hard constraints expressed as normal logic rules. We first focused on the special case represented by HMC problems, and proposed C-HMCNN(h), a novel model based on neural networks that (i) is able to leverage the hierarchical information to learn when to delegate the prediction on a superclass to one of its subclasses, (ii) produces predictions coherent by construction, and (iii) outperforms current state-of-the-art models on 20 commonly used real-world HMC benchmarks, and (iv) it can be easily implemented on GPUs using standard libraries. We then considered the general case and proposed CCN(h), which has four distinguishing features: (i) its predictions are always coherent with the given constraints, (ii) it can be implemented on GPUs using standard libraries, (iii) it extends C-HMCNN(h), and thus outperforms the state-of-the-art HMC models on HMC problems, and (iv) it outperforms the state-of-the-art MC models on 16 LCMC problems obtained adding automatically extracted constraints to well-known MC problems.

This work opens the path to many different lines of research. In general, the basic idea behind this article is to (i) incorporate the constraints in neural networks models guaranteeing their coherency, and (ii) exploit the constraints to improve performance. In this article, we focussed on MC problems with hard logical constraints on the output, but indeed the same idea can be applied also to other problems, and it could be interesting to investigate (i) whether it is possible to impose even more expressive constraints (e.g., involving also the input), (ii) how to incorporate both soft and hard constraints, and (iii) how to impose hard constraints on regression, binary classification, and multi-class classification problems.

Acknowledgments

This article is a revised and substantially extended version of the paper (Giunchiglia & Lukasiewicz, 2020). We thank Lei Feng, Francesco Giannini and Marco Gori for useful discussions. Eleonora Giunchiglia is supported by the EPSRC under the grant EP/N509711/1 and by an Oxford-DeepMind Graduate Scholarship. This work was also supported by the Alan Turing Institute under the EPSRC grant EP/N510129/1 and by the AXA Research Fund. We also acknowledge the use of the EPSRC-funded Tier 2 facility JADE (EP/P020275/1) and GPU computing support by Scan Computers International Ltd.

Appendix A. HMC - Experimental Analysis Details

In this section, we provide more details about the conducted experimental analysis for HMC problems. As stated in the article, across the different experiments, we kept all hyperparameters fixed with the exception of the hidden dimension and the learning rate, which are reported in the first two columns of Table 12. The other hyperparameters were determined by searching the best hyperparameters configuration on the Funcat datasets; we then took the configuration that led to the best results on the highest number of datasets. The hyperparameter values taken in consideration were: (i) learning rate: $[10^{-3}, 10^{-4}, 10^{-5}]$, (ii) batch size: $[4, 64, 256]$, (iii) dropout: $[0.6, 0.7]$, and (iv) weight decay: $[10^{-3}, 10^{-5}]$. Concerning the hidden dimension, we took into account all possible dimensions from 250 to 2000 with step equal to 250, and from 2000 to 10000 with step 1000. All experiments were run on an Nvidia Titan Xp with 12 GB memory.

In the last two columns of Table 12, we compare CCN(h)'s average inference time per batch in milliseconds when run on a CPU and on a GPU. The average is computed over 500 batches for each dataset. As it can be seen from the table, implementing CCN(h) on GPU led to much smaller inference times, especially on the GO datasets. For this experiment, we used an Nvidia Titan Xp with 12 GB memory as GPU and an Intel(R) Xeon(R) Gold 5218 CPU @ 2.30GHz as CPU. The hyperparameters of all neural networks were kept the same as in the other experiments.

Appendix B. LCMC - Experimental Analysis Details

In this section, we provide more details about the conducted experimental analysis for LCMC problems. As stated in the article, across the different experiments, we kept all hyperparameters fixed with the exception of the hidden dimension, which are reported in

Dataset	Hidden Dimension	Learning Rate	Time per batch (GPU)	Time per batch (CPU)
Cellcycle FUN	500	10^{-4}	2.0	24.5
Derisi FUN	500	10^{-4}	2.0	13.6
Eisen FUN	500	10^{-4}	1.7	14.6
Expr FUN	1000	10^{-4}	1.9	12.6
Gasch1 FUN	1000	10^{-4}	2.0	8.5
Gasch2 FUN	500	10^{-4}	2.8	8.7
Seq FUN	2000	10^{-4}	2.0	16.5
Spo FUN	250	10^{-4}	1.6	13.8
Cellcycle GO	1000	10^{-4}	2.4	715.1
Derisi GO	500	10^{-4}	2.5	668.8
Eisen GO	500	10^{-4}	3.4	571.1
Expr GO	4000	10^{-5}	3.9	751.6
Gasch1 GO	500	10^{-4}	2.5	788.3
Gasch2 GO	500	10^{-4}	2.8	752.2
Seq GO	9000	10^{-5}	2.6	837.8
Spo GO	500	10^{-4}	3.3	720.3
Diatoms	2000	10^{-5}	2.0	71.3
Enron	1000	10^{-5}	3.6	1.9
Imclef07a	1000	10^{-5}	3.4	9.9
Imclef07d	1000	10^{-5}	2.9	1.5

Table 12: Hidden dimension used for each dataset, learning rate used for each dataset, and average inference time per batch in milliseconds (ms). Average computed over 500 batches for each dataset.

Table 13. The other hyperparameters were determined by searching the best hyperparameters configuration on the validation sets; we then took the configuration that led to the best results on the highest number of datasets. The hyperparameter values taken in consideration were: (i) learning rate: $[10^{-3}, 10^{-4}, 10^{-5}]$, (ii) batch size: $[4, 64, 256]$, (iii) dropout: $[0.6, 0.7, 0.8]$, and (iv) weight decay: $[10^{-3}, 10^{-4}, 10^{-5}]$. Concerning the hidden dimension, we took into account all possible dimensions from 100 to 1000 with step equal to 100, and from 1000 to 5000 with step 500. Again, all experiments were run on an Nvidia Titan Xp with 12 GB memory.

Appendix C. Proof Theorem 2.7

Proof. Consider a data point and a class A.

$$\frac{\partial \text{CLoss}}{\partial h_A} = \sum_{B \in \mathcal{A}} \frac{\partial \text{CLoss}_B}{\partial h_A}.$$

Assume $y_A = 1$. For each class B such that $y_B = 0$:

$$\text{CLoss}_B = -\ln(1 - \text{CM}_B), \qquad \frac{\partial \text{CLoss}_B}{\partial h_A} = \frac{1}{1 - \text{CM}_B} \frac{\partial \text{CM}_B}{\partial h_A} = 0,$$

Dataset	Hidden Dimension
Arts	4000
Business	4000
Cal500	100
Emotions	100
Enron	2500
Genbase	5000
Image	1000
Medical	800
Rcv1Subset1	600
Rcv1Subset2	1500
Rcv1Subset3	4000
Rcv1Subset4	1000
Rcv1Subset5	4000
Science	2000
Scene	1500
Yeast	4000

Table 13: Hidden dimension used for each dataset.

because CM_B is not a function of h_A (since $y_A = 1$ and $y_B = 0$, $A \notin \mathcal{D}_B$), and hence $\frac{\partial \mathrm{CM}_B}{\partial h_A} = 0$. For each class B such that $y_B = 1$,

$$\mathrm{CLoss}_B = -\ln(\max_{C \in \mathcal{D}_B}(y_C h_C)), \qquad \frac{\partial \mathrm{CLoss}_B}{\partial h_A} = -\frac{1}{\max_{C\in\mathcal{D}_B}(y_C h_C)} \frac{\partial \max_{C\in\mathcal{D}_B}(y_C h_C)}{\partial h_A} \leq 0,$$

because if $\max_{C\in\mathcal{D}_B}(y_C h_C) = h_A$, then $\frac{\partial \mathrm{CLoss}_B}{\partial h_A} = -\frac{1}{h_A} \leq 0$, otherwise $\frac{\partial \mathrm{CLoss}_B}{\partial h_A} = 0$. Since $\frac{\partial \mathrm{CLoss}}{\partial h_A}$ is given by the sum of quantities that are smaller or equal zero, then $\frac{\partial \mathrm{CLoss}}{\partial h_A} \leq 0$.

Assume $y_A = 0$. For each class B such that $y_B = 0$:

$$\mathrm{CLoss}_B = -\ln(1 - \mathrm{CM}_B), \qquad \frac{\partial \mathrm{CLoss}_B}{\partial h_A} = \frac{1}{1 - \mathrm{CM}_B} \frac{\partial \mathrm{CM}_B}{\partial h_A} \geq 0,$$

because if $\mathrm{CM}_B = h_A$, then $\frac{\partial \mathrm{CM}_B}{\partial h_A} = 1$, otherwise $\frac{\partial \mathrm{CM}_B}{\partial h_A} = 0$. For each class B such that $y_B = 1$:

$$\mathrm{CLoss}_B = -\ln(\max_{C \in \mathcal{D}_B}(y_C h_C)), \qquad \frac{\partial \mathrm{CLoss}_B}{\partial h_A} = -\frac{1}{\max_{C\in\mathcal{D}_B}(y_C h_C)} \frac{\partial \max_{C\in\mathcal{D}_B}(y_C h_C)}{\partial h_A} = 0,$$

because $\max_{C\in\mathcal{D}_B}(y_C h_C) \neq h_A$, since $y_A = 0$. Since $\frac{\partial \mathrm{CLoss}}{\partial h_A}$ is given by the sum of quantities that are greater than or equal to zero, then $\frac{\partial \mathrm{CLoss}}{\partial h_A} \geq 0$. □

Appendix D. Proof Theorem 3.15

Proof. By induction on the number s of strata.

Assume $s = 1$. Then, the constraints in Π are definite rules, $\Pi_1 = \Pi$, and the statement follows.

Assume $s = n + 1 > 1$, and let $\mathcal{A}_1, \ldots, \mathcal{A}_{n+1}$ be the partition of the set $\mathcal{A}$ of classes computed by CompStrata(Π). By the induction hypothesis, $\Pi_1, \ldots, \Pi_n$ is a stratification of $\cup_{i=1}^{n} \Pi_i$ with the smallest number of strata. By construction, for each class A in $\mathcal{A}_{n+1}$ the path from a root to A in G_Π containing the maximum number of negative edges contains n negative edges. Thus, for each class $A \in \mathcal{A}_{n+1}$, there exists a constraint $r \in \Pi_{n+1}$ such that:

1. $\mathit{head}(r) = A$,
2. there exists a class $B \in \mathcal{A}_n$ such that $\neg B \in \mathit{body}^-(r)$.

Furthermore, $\Pi = \cup_{i=1}^{n+1} \Pi_i$ is stratified, since $\cup_{i=1}^{n} \Pi_i$ is stratified by the induction hypothesis and, for every constraint $r \in \Pi_{n+1}$,

1. each class in $\mathit{body}^+(r)$ belongs to $\cup_{i=1}^{n+1} \mathcal{A}_i$, and
2. each class in $\mathit{body}^-(r)$ belongs to $\cup_{i=1}^{n} \mathcal{A}_i$.

Since $\Pi_1, \ldots, \Pi_n$ is a stratification of $\cup_{i=1}^{n} \Pi_i$ with the smallest number of strata, then $\Pi_1, \ldots, \Pi_{n+1}$ is a stratification of Π with the smallest number of strata. $\square$

Appendix E. Proof Theorem 3.17

Proof. Let $\mathcal{A}_1, \ldots, \mathcal{A}_s$ be the partition of $\mathcal{A}$ computed by CompStrata(Π). We recall that, for a class A, (15) is

$$m_A = \max(h_A, m_A^{r_1}, \ldots, m_A^{r_p}),$$

where $r_1, \ldots, r_p$ are all the constraints in Π with head A and, for each such constraint r_j of form (9),

$$m_A^{r_j} = \min(m_{A_1}, \ldots, m_{A_k}, \overline{m}_{A_{k+1}}, \ldots, \overline{m}_{A_n}).$$

Consider a generic class $A \in \mathcal{A}_i$. We show that the definition of CM_A is equal to the expression resulting from the substitution of each m_{A_l} in $m_A^{r_j}$ $(1 \leq j \leq p)$ with

1. CM_{A_l} if $A_l \in \cup_{j=1}^{i-1} \mathcal{A}_j$,
2. the right-hand side of Equation (18) if $A_l \in \mathcal{A}_i$.

Consider the result of such a substitution in $m_A^{r_j}$. Applying the distributivity of the minimum operation over the maximum operation, we get

$$m_A^{r_j} = \max_{r \in \Pi_i^*(r_j)} (\min(v_{\mathit{body}(r)})),$$

where

1. $\Pi_i^*(r_j)$ is the set of constraints initially equal to $\{r_j\}$ and then obtained by recursively adding the constraints obtained from a constraint $r \in \Pi_i^*(r_j)$ by substituting a class $B \in \mathit{body}^+(r) \cap \mathcal{A}_i$ with $\mathit{body}(r')$ for any constraint r' with $\mathit{head}(r') = B$, and

2. $v_{body(r)}$ is the set

$$\{\mathrm{CM}_B : B \in body^+(r), B \in \cup_{j=1}^{i-1}\mathcal{A}_j\} \cup \\ \{h_B : B \in body^+(r), B \in \mathcal{A}_i\} \cup \\ \{\overline{\mathrm{CM}}_B : \neg B \in body^-(r)\}.$$

Since the set of constraints in Π_i^* with head A is equal to $\cup_{j=1}^{p}\Pi_i^*(r_j)$, the statement follows. □

Appendix F. Proof Theorem 3.18

Proof. We recall that, for each class A, $\mathrm{CCN}(h)_A = \mathrm{CM}_A$, and we use CM_A, since shorter.

Consider the partition $\mathcal{A}_1, \dots, \mathcal{A}_s$ of the set of classes $\mathcal{A}$ and the corresponding stratification $\Pi_1, \dots, \Pi_s$ of Π. We prove that the outputs of CM for the classes in $\mathcal{A}_i$ are the smallest values satisfying (15), given the values CM_B for $B \in \cup_{j=1}^{i-1}\mathcal{A}_j$.

If a model satisfies (15), then it also satisfies the inequalities (10) associated with each constraint (9) in Π_i. Thus, we first prove that for any model m satisfying (10) for each constraint (9) in Π_i, given the values m_B for $B \in \cup_{j=1}^{i-1}\mathcal{A}_j$, $m_A \geq \mathrm{CM}_A$. This allows us to conclude that any model m satisfying (15) has values bigger than or equal to those of CM.

Let $I(\Pi_i)$ be the set of inequalities (10), one for each constraint of the form (9) in Π_i union, for each class $A \in \mathcal{A}_i$,

$$h_A \leq m_A. \tag{20}$$

We represent $I(\Pi_i)$ as the set of pairs $\langle \mathcal{S}, m_A \rangle$, where $\mathcal{S}$ is the set $\{m_{A_1}, \dots, \overline{m}_{A_n}\}$ (resp., $\{h_A\}$) in the case of (10) (resp., (20)).

Define $I^*(\Pi_i)$ to be the set of inequalities obtained from $I(\Pi_i)$ by recursively adding the pairs $\langle \mathcal{S} \cup \mathcal{S}' \setminus A, m_B \rangle$ such that $\langle \mathcal{S}, m_A \rangle \in I^*(\Pi_i)$, $\langle \mathcal{S}', m_B \rangle \in I^*(\Pi_i)$ and $A \in \mathcal{S}'$. $I^*(\Pi_i)$ is finite, and each inequality in $I^*(\Pi_i)$ is entailed by the inequalities in $I(\Pi_i)$. Thus, $I^*(\Pi_i)$ and $I(\Pi_i)$ have the same set of solutions. For each constraint r in Π_i^* of the form (9) with head $A \in \mathcal{A}_i$, the inequality

$$\langle \{v_{A_1}, \dots, v_{A_k}, \overline{m}_{A_{k+1}}, \dots, \overline{m}_{A_n}\}, A \rangle \tag{21}$$

belongs to $I^*(\Pi_i)$, where $v_{A_1} = h_{A_1}$ if $A_1 \in \mathcal{A}_i$, and $v_{A_1} = m_{A_1}$ if $A_1 \in \cup_{j=1}^{i-1}\mathcal{A}_j$. Analogously for $v_{A_2}, \dots, v_{A_k}$.

By definition, CM_A is the smallest value satisfying the inequalities (21) in $I^*(\Pi_i)$. Thus, for any model m satisfying $I^*(\Pi_i)$, $m_A \geq \mathrm{CM}_A$. □

Appendix G. Proof Theorem 3.19

Proof. We prove each statement of the theorem separately. By hypothesis, $\mathcal{H}$ is the set of classes A such that $h_A > \theta$. $\mathcal{M}$ is the set of classes A such that $\mathrm{CM}_A > \theta$. $\mathcal{A}_1, \dots, \mathcal{A}_s$ and $\Pi_1, \dots, \Pi_s$ is the partition of $\mathcal{A}$ and Π computed by CompStrata(Π), respectively.

1. CCN(h) extends the set of classes associated with x by h. We have to prove that $\mathcal{H} \subseteq \mathcal{M}$. $A \in \mathcal{H}$ iff $h_A > \theta$. Since $\mathrm{CM}_A \geq h_A$, if $A \in \mathcal{H}$, then $A \in \mathcal{M}$.

   $\mathcal{M}$ is coherent with Π. We have to prove that for each constraint r of the form (9), if $\min(\mathrm{CM}_{A_1}, \dots, \mathrm{CM}_{A_k}, \overline{\mathrm{CM}}_{A_{k+1}}, \dots, \overline{\mathrm{CM}}_{A_n}) > \theta$, then $\mathrm{CM}_A > \theta$, which is an easy consequence of the fact that the outputs of CM satisfy (15) and thus also (10).

2. $\mathcal{M}$ is supported relative to $\mathcal{H}$ and Π. Assume it is not. Then, consider a class $A \in \mathcal{M} \setminus \mathcal{H}$ such that for each constraint $r \in \Pi$ of the form (9), there exists an index $j \in \{1, \ldots, n\}$ such that
   (a) both $\mathrm{CM}_{A_j} \leq \theta$ and $j = 1, \ldots, k$, or
   (b) both $\overline{\mathrm{CM}}_{A_j} \leq \theta$ and $j = k+1, \ldots, n$.

   By Theorem 3.17, CM_A is the smallest value satisfying Equation (15) given the values m_B for $B \in \cup_{j=1}^{i-1} \mathcal{A}_j$. Thus, $\mathrm{CM}_A > \theta$ is not possible, and this contradicts $A \in \mathcal{M}$.

3. $\mathcal{M}$ is minimal relative to $\mathcal{H}$ and Π. Let $\mathcal{M}_0 = \mathcal{H}$. Let $\mathcal{M}_{i+1}$ be the closure of $\mathcal{M}_i$ under Π^*_{i+1} $(1 \leq i < s)$. The statement is a consequence of the minimality of each $\mathcal{M}_{i+1}$ and the fact that $\mathcal{M} = \mathcal{M}_s$.

4. $\mathcal{M}$ is the unique set satisfying all the previous properties. As above, let $\mathcal{M}_0 = \mathcal{H}$, and let $\mathcal{M}_{i+1}$ be the closure of $\mathcal{M}_i$ under Π^*_{i+1} $(1 \leq i < s)$. The statement is a consequence of the uniqueness of each $\mathcal{M}_{i+1}$ and the fact that $\mathcal{M} = \mathcal{M}_s$.

□

Appendix H. Proof Theorem 3.22

Proof. First, observe that if Π is stratified, then also $\Pi \cup \{\to A : A \in \mathcal{H}\}$ is stratified. The theorem is an easy consequence of the fact that in the case of a stratified set of constraints, the stable and the canonical model semantics coincide (see, e.g., Gelfond & Lifschitz, 1988), and the latter, for $\Pi \cup \{\to A : A \in \mathcal{H}\}$, is defined as follows.

Consider the partition $\mathcal{A}_1, \ldots, \mathcal{A}_s$ of the set of classes $\mathcal{A}$ and the corresponding stratification $\Pi_1, \ldots, \Pi_s$ resulting from CompStrata(Π). Define $\mathcal{M}_0 = \mathcal{H}$, and, for each $0 \leq i < s$,

$$\mathcal{M}_{i+1} = T(\mathcal{M}_i, \Pi_{i+1}^{\mathcal{M}_i}),$$

where $T(\mathcal{M}_i, \Pi_{i+1}^{\mathcal{M}_i})$ is the smallest superset of $\mathcal{M}_i$ closed under the reduct $\Pi_{i+1}^{\mathcal{M}_i}$ of Π_{i+1} relative to $\mathcal{M}_i$. $\mathcal{M}_{i+1}$ is unique.

Then, the canonical model $\mathcal{M}$ of $\Pi \cup \{\to A : A \in \mathcal{H}\}$ is $\mathcal{M} = \mathcal{M}_s$. □

Appendix I. Proof Theorem 3.24

Proof. Consider a data point and a class A.

$$\frac{\partial \mathrm{CLoss}}{\partial h_A} = \sum_{B \in \mathcal{A}} \frac{\partial \mathrm{CLoss}_B}{\partial h_A}.$$

We consider only the case $y_A = 1$ (the case $y_A = 0$ is analogous). Consider a class B.

1. If $y_B = 1$,

$$\mathrm{CLoss}_B = -\ln(\mathrm{CM}_B^+), \qquad \frac{\partial \mathrm{CLoss}_B}{\partial h_A} = -\frac{1}{\mathrm{CM}_B^+} \frac{\partial \mathrm{CM}_B^+}{\partial h_A} \leq 0,$$

   because:

- either $\text{CM}^+_B = h_A$ (which is possible only if $A = B$, or there exists a constraint r with head B such that $h^{+,r}_B = h_A$) and then $\frac{\partial \text{CLoss}_B}{\partial h_A} = -\frac{1}{h_A} \leq 0$,
- or CM^+_B is a value not dependent on h_A and then $\frac{\partial \text{CLoss}_B}{\partial h_A} = 0$ (since $y_A = 1$, it cannot be the case that there exists a constraint r with head B such that $h^{+,r}_B = \overline{h}_A$).

2. if $y_B = 0$,

$$\text{CLoss}_B = -\ln(\overline{\text{CM}^-_B}), \qquad \frac{\partial \text{CLoss}_B}{\partial h_A} = \frac{1}{\overline{\text{CM}^-_B}} \frac{\partial \text{CM}^-_B}{\partial h_A} \leq 0,$$

because:

- either $\text{CM}^-_B = \overline{h}_A$ (which is possible only if $A = B$ or there exists a constraint r with head B such that $h^{-,r}_B = \overline{h}_A$) and then $\frac{\partial \text{CLoss}_B}{\partial h_A} = -\frac{1}{h_A} \leq 0$,
- or CM^-_B is a value not dependent on h_A and then $\frac{\partial \text{CLoss}_B}{\partial h_A} = 0$ (since $y_A = 1$, it cannot be the case that there exists a constraint r with head B such that $h^{-,r}_B = h_A$).

Since $\frac{\partial \text{CLoss}}{\partial h_A}$ is the sum of quantities that are at most zero, then $\frac{\partial \text{CLoss}}{\partial h_A} \leq 0$. □

References

Agrawal, R., & Srikant, R. (1994). Fast algorithms for mining association rules in large databases. In *Proceedings of VLDB*, pp. 487–499.

Apt, K. R., Blair, H. A., & Walker, A. (1988). Towards a theory of declarative knowledge. In Minker, J. (Ed.), *Foundations of Deductive Databases and Logic Programming*, pp. 89–148. Morgan Kaufmann.

Barutcuoglu, Z., Schapire, R. E., & Troyanskaya, O. G. (2006). Hierarchical multi-label prediction of gene function. *Bioinformatics*, *22*(7), 830–836.

Benavoli, A., Corani, G., & Mangili, F. (2016). Should we really use post-hoc tests based on mean-ranks?. *Journal of Machine Learning Research*, *17*(5), 1–10.

Bertsekas, D. P. (2014). *Constrained Optimization and Lagrange Multiplier Methods*. Academic Press.

Bi, W., & Kwok, J. T. (2011). Multi-label classification on tree- and DAG-structured hierarchies. In *Proceedings of ICML*, pp. 17–24.

Borges, H. B., & Nievola, J. C. (2012). Multi-label hierarchical classification using a competitive neural network for protein function prediction. In *Proceedings of IJCNN*.

Boutell, M. R., Luo, J., Shen, X., & Brown, C. M. (2004). Learning multi-label scene classification. *Pattern Recognition*, *37*(9).

Cerri, R., Barros, R. C., & de Leon Ferreira de Carvalho, A. C. P. (2011). Hierarchical multi-label classification for protein function prediction: A local approach based on neural networks. In *Proceedings of ISDA*, pp. 337–343.

Cerri, R., Barros, R. C., & de Leon Ferreira de Carvalho, A. C. P. (2014). Hierarchical multi-label classification using local neural networks. *Journal of Computer and System Sciences*, *80*(1), 39–56.

Cerri, R., Barros, R. C., de Leon Ferreira de Carvalho, A. C. P., & Jin, Y. (2016). Reduction strategies for hierarchical multi-label classification in protein function prediction. *BMC Bioinformatics*, *17*, 373.

Cesa-Bianchi, N., Gentile, C., & Zaniboni, L. (2006). Incremental algorithms for hierarchical classification. *Journal of Machine Learning Research*, *7*, 31–54.

Chen, L.-C., Schwing, A., Yuille, A., & Urtasun, R. (2015). Learning deep structured models. In *Proceedings of ICML*, pp. 1785–1794.

Choi, Y., Vergari, A., & den Broeck, G. V. (2020). Probabilistic circuits: Representation and inference.. Last accessed 09 August 2021.

Clare, A. (2003). *Machine Learning and Data Mining for Yeast Functional Genomics*. Ph.D. thesis, University of Wales.

Cormen, T. H., Leiserson, C. E., Rivest, R. L., & Stein, C. (2009). *Introduction to Algorithms, 3rd Edition*. MIT Press.

Demsar, J. (2006). Statistical comparisons of classifiers over multiple data sets. *Journal of Machine Learning Research*, *7*, 1–30.

Deng, J., Ding, N., Jia, Y., Frome, A., Murphy, K., Bengio, S., Li, Y., Neven, H., & Adam, H. (2014). Large-scale object classification using label relation graphs. In *Proceedings of ECCV*, Vol. 8689, pp. 48–64.

Deng, J., Dong, W., Socher, R., Li, L., Li, K., & Li, F. (2009). ImageNet: A large-scale hierarchical image database. In *Proceedings of CVPR*, pp. 248–255.

Diligenti, M., Gori, M., & Sacca, C. (2017). Semantic-based regularization for learning and inference. *Artificial Intelligence*, *244*, 143–165.

Dimitrovski, I., Kocev, D., Loskovska, S., & Džeroski, S. (2008). Hierchical annotation of medical images. In *Proceedings of IS*, pp. 174–181.

Dimitrovski, I., Kocev, D., Loskovska, S., & Dzeroski, S. (2012). Hierarchical classification of diatom images using ensembles of predictive clustering trees. *Ecological Informatics*, *7*(1), 19–29.

Diplaris, S., Tsoumakas, G., Mitkas, P. A., & Vlahavas, I. (2005). Protein classification with multiple algorithms. In Bozanis, P., & Houstis, E. N. (Eds.), *Advances in Informatics*.

Donadello, I., Serafini, L., & d'Avila Garcez, A. (2017). Logic tensor networks for semantic image interpretation. In *Proceedings of IJCAI*, pp. 1596–1602.

Elisseeff, A., & Weston, J. (2001). A kernel method for multi-labelled classification. In *Proceedings of NeurIPS*, p. 681–687.

Farina, F., Melacci, S., Garulli, A., & Giannitrapani, A. (2020). Asynchronous distributed learning from constraints. *IEEE Transactions on Neural Networks and Learning Systems*, *31*(10), 4367–4373.

Feng, L., An, B., & He, S. (2019). Collaboration based multi-label learning. In *Proceedings of AAAI*, pp. 3550–3557.

Feng, S., Fu, P., & Zheng, W. (2018). A hierarchical multi-label classification method based on neural networks for gene function prediction. *Biotechnology and Biotechnological Equipment*, *32*, 1613–1621.

Fletcher, R. (2013). *Practical Methods of Optimization.* John Wiley & Sons.

Gelfond, M., & Lifschitz, V. (1988). The stable model semantics for logic programming. In *Proceedings of Logic Programming*, pp. 1070–1080.

Giunchiglia, E., & Lukasiewicz, T. (2020). Coherent hierarchical multi-label classification networks. In *Proceedings of NeurIPS*, pp. 9662–9673.

Gnecco, G., Gori, M., Melacci, S., & Sanguineti, M. (2014). Learning with mixed hard/soft pointwise constraints. *IEEE Transactions on Neural Networks and Learning Systems*, *26*(9), 2019–2032.

Hochreiter, S., & Schmidhuber, J. (1997). Long short-term memory. *Neural Computation*, *9*(8), 1735–1780.

Hu, Z., Ma, X., Liu, Z., Hovy, E., & Xing, E. (2016a). Harnessing deep neural networks with logic rules. In *Proceedings of ACL*, pp. 2410–2420.

Hu, Z., Yang, Z., Salakhutdinov, R., & Xing, E. (2016b). Deep neural networks with massive learned knowledge. In *Proceedings of EMNLP*, pp. 1670–1679.

Huang, X., Kroening, D., Ruan, W., Sharp, J., Sun, Y., Thamo, E., Wu, M., & Yi, X. (2020). A survey of safety and trustworthiness of deep neural networks: Verification, testing, adversarial attack and defence, and interpretability. *Computer Science Review*, *37*.

Huang, Z., Xu, W., & Yu, K. (2015). Bidirectional LSTM-CRF models for sequence tagging. *ArXiv*, *abs/1508.01991*.

Kingma, D. P., & Ba, J. (2015). Adam: A method for stochastic optimization. In *Proceedings of ICLR*.

Kisa, D., den Broeck, G. V., Choi, A., & Darwiche, A. (2014). Probabilistic sentential decision diagrams. In Baral, C., Giacomo, G. D., & Eiter, T. (Eds.), *Proceedings of KR*. AAAI Press.

Klimt, B., & Yang, Y. (2004). The Enron Corpus: A new dataset for email classification research. In *Proceedings of ECML*, pp. 217–226.

Kulmanov, M., Khan, M. A., & Hoehndorf, R. (2018). DeepGO: Predicting protein functions from sequence and interactions using a deep ontology-aware classifier. *Bioinformatics*, *34*(4), 660–668.

Lewis, D. D., Yang, Y., Rose, T. G., & Li, F. (2004). RCV1: A new benchmark collection for text categorization research. *Journal of Machine Learning Research*, *5*, 361–397.

Li, T., & Srikumar, V. (2019). Augmenting neural networks with first-order logic. In *Proceedings of ACL*, pp. 292–302.

Li, Y., Wang, S., Umarov, R., Xie, B., Fan, M., Li, L., & Gao, X. (2018). DEEPre: Sequence-based enzyme EC number prediction by deep learning. *Bioinformatics*, *34*(5).

Lloyd, J. W. (1987). *Foundations of Logic Programming, 2nd Edition.* Springer.

Lomuscio, A., & Maganti, L. (2017). An approach to reachability analysis for feed-forward relu neural networks. *CoRR*, *abs/1706.07351*.

Luenberger, D. G. (1997). *Optimization by Vector Space Methods.* John Wiley & Sons.

Ma, L., Juefei-Xu, F., Zhang, F., Sun, J., Xue, M., Li, B., Chen, C., Su, T., Li, L., Liu, Y., Zhao, J., & Wang, Y. (2018). Deepgauge: multi-granularity testing criteria for deep learning systems. In *Proceedings of ACM/IEEE ASE*, pp. 120–131. ACM.

Masera, L., & Blanzieri, E. (2018). AWX: An integrated approach to hierarchical-multilabel classification. In *Proceedings of ECML-PKDD*, pp. 322–336.

Metcalfe, G. (2005). Fundamentals of fuzzy logics. https://www.logic.at/tbilisi05/Metcalfe-notes.pdf.

Nakano, F. K., Lietaert, M., & Vens, C. (2019). Machine learning for discovering missing or wrong protein function annotations — A comparison using updated benchmark datasets. *BMC Bioinformatics*, *20*(1), 485:1–485:32.

Obozinski, G., Lanckriet, G. R. G., Grant, C. E., Jordan, M. I., & Noble, W. S. (2008). Consistent probabilistic outputs for protein function prediction. *Genome Biology*, *9*.

Pedregosa, F., Varoquaux, G., Gramfort, A., Michel, V., Thirion, B., Grisel, O., Blondel, M., Prettenhofer, P., Weiss, R., Dubourg, V., Vanderplas, J., Passos, A., Cournapeau, D., Brucher, M., Perrot, M., & Duchesnay, E. (2011). Scikit-learn: Machine learning in Python. *Journal of Machine Learning Research*, *12*, 2825–2830.

Pei, K., Cao, Y., Yang, J., & Jana, S. (2019). Deepxplore: automated whitebox testing of deep learning systems. *Communications ACM*, *62*(11), 137–145.

Pereira, R. B., Plastino, A., Zadrozny, B., & Merschmann, L. H. (2018). Correlation analysis of performance measures for multi-label classification. *Information Processing & Management*, *54*(3), 359 – 369.

Pestian, J. P., Brew, C., Matykiewicz, P., Hovermale, D. J., Johnson, N., Cohen, K. B., & Duch, W. (2007). A shared task involving multi-label classification of clinical free text. In *Proceedings of Workshop on BioNLP*.

Poon, H., & Domingos, P. (2011). Sum-product networks: A new deep architecture. In *2011 IEEE International Conference on Computer Vision Workshops (ICCV Workshops)*, pp. 689–690.

Pulina, L., & Tacchella, A. (2010). An abstraction-refinement approach to verification of artificial neural networks. In *Proceedings of CAV*, pp. 243–257.

Rahman, T., Kothalkar, P., & Gogate, V. (2014). Cutset networks: A simple, tractable, and scalable approach for improving the accuracy of chow-liu trees. In Calders, T., Esposito, F., Hüllermeier, E., & Meo, R. (Eds.), *Machine Learning and Knowledge Discovery in Databases*, pp. 630–645, Berlin, Heidelberg. Springer Berlin Heidelberg.

Read, J., Pfahringer, B., Holmes, G., & Frank, E. (2009). Classifier chains for multi-label classification. In Buntine, W., Grobelnik, M., Mladenić, D., & Shawe-Taylor, J. (Eds.), *Machine Learning and Knowledge Discovery in Databases*, pp. 254–269, Berlin, Heidelberg. Springer Berlin Heidelberg.

Read, J., Pfahringer, B., & Holmes, G. (2008). Multi-label classification using ensembles of pruned sets. In *Proceedings of IEEE ICDM*.

Rousu, J., Saunders, C., Szedmák, S., & Shawe-Taylor, J. (2006). Kernel-based learning of hierarchical multilabel classification models. *Journal of Machine Learning Research*, *7*, 1601–1626.

Saito, T., & Rehmsmeier, M. (2015). The precision-recall plot is more informative than the roc plot when evaluating binary classifiers on imbalanced datasets. *PLOS ONE*, *10*(3), 1–21.

Schietgat, L., Vens, C., Struyf, J., Blockeel, H., Kocev, D., & Dzeroski, S. (2010). Predicting gene function using hierarchical multi-label decision tree ensembles. *BMC Bioinformatics*, *11*, 2.

Shen, Y., Choi, A., & Darwiche, A. (2016). Tractable operations for arithmetic circuits of probabilistic models. In Lee, D., Sugiyama, M., Luxburg, U., Guyon, I., & Garnett, R. (Eds.), *Proceedings of NeurIPS*. Curran Associates, Inc.

Shen, Y., Choi, A., & Darwiche, A. (2018). Conditional psdds: Modeling and learning with modular knowledge. In McIlraith, S. A., & Weinberger, K. Q. (Eds.), *Proceedings of AAAI*, pp. 6433–6442.

Shen, Y., Goyanka, A., Darwiche, A., & Choi, A. (2019). Structured bayesian networks: From inference to learning with routes. In *Proceedings of AAAI*, pp. 7957–7965.

Silla, C. N. J., & Freitas, A. A. (2011). A survey of hierarchical classification across different application domains. *Data Mining and Knowledge Discovery*, *22*(1-2), 31–72.

Spolaôr, N., Cherman, E. A., Metz, J., & Monard, M. C. (2013). A systematic review on experimental multi-label learning. Tech. rep. 362, Institute of Mathematics and Computational Sciences, University of São Paulo.

Srivastava, A. N., & Zane-Ulman, B. (2005). Discovering recurring anomalies in text reports regarding complex space systems. In *Proceedings of IEEE Aerospace Conference*.

Stewart, R., & Ermon, S. (2017). Label-free supervision of neural networks with physics and domain knowledge. In *Proceedings of AAAI*, pp. 2576–2582.

Szymanski, P., & Kajdanowicz, T. (2017). A scikit-based python environment for performing multi-label classification. *CoRR*, *abs/1702.01460*.

Tsoumakas, G., Dimou, A., Spyromitros, E., Mezaris, V., Kompatsiaris, I., & Vlahavas, I. (2009). Correlation-based pruning of stacked binary relevance models for multi-label learning. In *Proceedings of International Workshop on Learning from Multi-label Data*.

Tsoumakas, G., Katakis, I., & Vlahavas, I. (2008). Effective and efficient multilabel classification in domains with large number of labels. In *Proceedings of ECML/PKDD — Workshop on Mining Multidimensional Data*.

Tsoumakas, G., & Vlahavas, I. (2007). Random k-labelsets: An ensemble method for multilabel classification. In Kok, J. N., Koronacki, J., Mantaras, R. L. d., Matwin, S., Mladenič, D., & Skowron, A. (Eds.), *Proceedings of ECML*, Berlin, Heidelberg. Springer Berlin Heidelberg.

Turnbull, D., Barrington, L., Torres, D., & Lanckriet, G. (2008). Semantic annotation and retrieval of music and sound effects. *IEEE Transactions on Audio, Speech, and Language Processing*, *16*(2), 467–476.

Valentini, G. (2011). True path rule hierarchical ensembles for genome-wide gene function prediction. *IEEE/ACM IEEE/ACM Transactions on Computational Biology and Bioinformatics*, *8*(3), 832–847.

Vens, C., Struyf, J., Schietgat, L., Dzeroski, S., & Blockeel, H. (2008). Decision trees for hierarchical multi-label classification. *Machine Learning*, *73*(2), 185–214.

Wehrmann, J., Cerri, R., & Barros, R. C. (2018). Hierarchical multi-label classification networks. In *Proceedings of ICML*, pp. 5225–5234.

Xu, C., & Geng, X. (2019). Hierarchical classification based on label distribution learning. In *Proceedings of AAAI*, pp. 5533–5540.

Xu, J., Zhang, Z., Friedman, T., Liang, Y., & Van den Broeck, G. (2018). A semantic loss function for deep learning with symbolic knowledge. In *Proceedings of ICML*.

Zhang, M.-L., & Zhou, Z.-H. (2007). Ml-knn: A lazy learning approach to multi-label learning. *Pattern Recognition*, *40*(7), 2038 – 2048.

Zou, Z., Tian, S., Gao, X., & Li, Y. (2019). mlDEEPre: Multi-functional enzyme function prediction with hierarchical multi-label deep learning. *Frontiers in Genetics*, *9*.